*Vision Res.* Vol. 32, No. 7, pp. 1297–1318, 1992
Printed in Great Britain. 

0042-6989/92 $5.00 + 0.00


# The Effect of Adaptation on the Differential Sensitivity of the *S*-cone Color System

QASIM ZAIDI,* ARTHUR SHAPIRO,* DONALD HOOD*

*Received 6 May 1991; in revised form 24 September 1991*

**This paper presents a psychophysical dissection of the *S*-cone color system. Experiments were guided by a skeletal model that assumed a first stage consisting of *S*-, *M*- and *L*-cones, and a second stage of the opponent combination of the *S* and $L + M$ signals. The response of the *S*-cone system was isolated by measuring difference thresholds between lights that were equiluminant tritanopic confusion pairs and thus differed only in *S*-cone excitation. Two types of mechanisms that control sensitivity in the *S*-cone system were identified: (i) static mechanisms that have a restricted range and thus limit discrimination to a small range of inputs; and (ii) adaptive mechanisms that change the state of the system in response to changes in steady illumination, so that the system is sensitive to small changes from the adapting light. These mechanisms were localized by lights that stimulated the *S*-cone system while keeping the signal constant at either the *S*, the $L + M$, or the post-opponent stage. The response function of the static mechanism was estimated by measuring difference thresholds at judgment points other than the steady adapting light. This procedure was repeated at a number of adaptation lights to examine the properties of adaptive mechanisms. The data were consistent with an elaborated model that included identical multiplicative gain control mechanisms in the *S* and $L + M$ pre-opponent branches, and a post-opponent static sigmoidal nonlinearity with different amounts of compression for positive and negative opponent inputs.**

Visual adaptation Color vision Opponent-mechanisms *S*-cone system Gain control Response non-linearity Visual sensitivity

## INTRODUCTION

The present study had two interwined goals. The first goal was to understand more about the part of the visual system that is driven by short-wavelength-sensitive (*S*)-cones. It is generally thought that *S*-cone signals are processed either exclusively, or predominantly, by a chromatic system that responds to the difference between the signal of the *S*-cones and that of the long-wavelength-sensitive (*L*)- and middle-wavelength-sensitive (*M*)-cones (Boynton, 1979; Stockman, Macleod & Depriest, 1991). This system was originally identified by Hering (1878) as the "yellow–blue" hue system with a null response to "unique-red" and "unique-green" colors. In zone theories (Donders, 1881; von Kries, 1905), the "yellow–blue" system was one of the three second-stage mechanisms of color vision, and its response was expressed as a linear opponent combination of cone signals. Schrodinger (1925) showed that linearity of the system required that all "null" colors, including "unique-red", "achromatic-white" and "unique-green", should fall on a straight line in a chromaticity diagram. Dimmick and Hubbard (1939a, b) used a hue cancellation procedure to show that the chromaticities of these hues were not colinear and hence the response of this system could not be expressed as a linear combination of cone signals. Since then, a number of investigators have modeled "yellow–blue" opponency as a nonlinear combination of the relative cone absorptions (Larimer, Krantz & Cicerone, 1975; Werner & Wooten, 1979; Pokorny, Smith, Burns, Elsner & Zaidi, 1981; Burns, Elsner, Pokorny & Smith, 1984). Because the state of adaptation is not considered explicitly in these models, it is not clear whether the nonlinearity is due to an opponent stage that combines signals in a nonlinear fashion, to changes in the adaptation state of pre- or post-opponent stages, or to a nonlinear response function at one or more stages. In addition, unlike threshold measurements, hue judgments cannot be linked to the properties of underlying mechanisms in a rigorous manner (Brindley, 1970).

A simpler picture of the form of opponent combination was presented by Krauskopf, Williams and Heely (1982) on the basis of sensitivity measurements. By measuring selectivity of threshold elevations following habituation to prolonged temporal modulation of colors, they identified three independent "cardinal" directions in color space. These directions were: a pure *S*-cone direction where the excitation of the *L*- and

*Department of Psychology, Columbia University, New York, NY 10027, U.S.A.

$M$-cones was constant, a $L-M$ direction where $L+M$- and $S$-cone excitation was constant, and a $S+L+M$ direction passing through mid-white. A simple mechanistic scheme compatible with the results consists of three second-stage mechanisms, each with a null response to two of the cardinal directions. The spectral response of each "cardinal" mechanism is described as a linear combination of relative cone absorptions. The mechanism that responds to exclusive modulation of $S$-cone excitation, but not to modulation in the other cardinal directions, will be referred to as the $S$-cone cardinal mechanism. Based on these results, it seems probable that in the $S$-cone system the opponent combination rule is linear and that nonlinearities are due to other processes. In this study, adaptation processes, response functions, and rules of signal combination were all investigated.

The second goal of this study was to learn more about the processes that control sensitivity in the visual system by examining their effect in an experimentally isolated sub-system. Using a variety of procedures, a number of investigators have shown that an observer adapted to a steady light can best discriminate between lights similar to the adapting light. Craik (1938) and Heinemann (1961) found that differential brightness thresholds were lowest at the brightness to which an observer was adapted. Similarly, Brown (1952), Hurvich and Jameson (1961), Pointer (1974) and Loomis and Berger (1979) found that chromatic discrimination thresholds were smaller when the test field was surrounded by a field of a similar chromaticity than when it was surrounded by light of a markedly different color. Because of the ability to adapt, an observer can reliably discriminate small changes from the adapting light over a larger range of lighting conditions than would be possible otherwise. Lythgoe (1936) compared this capacity of the visual system to the operation of an ammeter: at any setting there is only a restricted range of currents that fall within the scale of an ammeter, but currents outside of this range can be measured by adjusting the gain. The adaptation is not instantaneous. After a change from one steady light to another, thresholds are largest at the onset of the change and then steadily decrease as the observer adapts to the new light (Crawford, 1946).

To account for this ability, Craik (1938) and Stiles (1967) implicitly divided the mechanisms that control differential sensitivity into two fundamental types: the first type limit sensitivity because their responses to test lights can vary only within a restricted range, whereas the second type change the range of sensitivity as a function of the adapting light. These two types of mechanisms have been formalized in mathematical models by Geisler (1978, 1979, 1981, 1983), Hood (1978), Ilves, Maurer, Wandell and Buckingham (1978), Hood, Finkelstein and Buckingam (1979), Finkelstein and Hood (1981), Finkelstein, Harrison and Hood (1990), Dawis (1981), Hood and Greenstein (1982), Adelson (1982) and Hayhoe, Benimoff and Hood (1987). In these models, in any state of adaptation, sensitivity is assumed to be limited by "static" mechanisms, whose response is a nonlinear compressive function of the instantaneous input and is unaffected by the history of light exposure, whereas the gain (*output/input*) of the "adaptive" mechanisms is assumed to be sluggishly dependent on the history of light exposure. In this study, an explicit model based on these two types of mechanisms was used to explain empirical results from experiments on the sensitivity of the $S$-cone system.

Attempts to isolate the properties of a color system by measurements of differential color discrimination generally follow the tradition of the two-color increment threshold experiments of Stiles (1939, 1949, 1953, 1959, 1978). However, despite Stiles' elegant theory and precise methodology, his experiments were unsuccessful in their original aim of identifying the independent mechanisms of trichromacy. In 1953, Stiles started using the neutral term "$\Pi$ mechanisms" in lieu of the terms "red", "green" and "blue" that he had used previously. Later investigators (Guth & Lodge, 1973; Pugh, 1976; Ingling, 1977; Mollon & Polden, 1977) used variants of Stiles' procedure to show inhibition between different classes of cones at a second stage. Based on the results of these studies, it is clear that for most spatio-temporal stimulus configurations, increment threshold procedures will not isolate the spectral properties of mechanisms at any particular level of the visual system. Sensitivity to an increment in the presence of a background can be limited by any of the levels of the color system that is most sensitive to the difference in signals from the increment and the background. When the spectral composition of the increment or the background is changed, the change in threshold could reflect the spectral property of any level, making it difficult to isolate a single level of a targeted mechanism. Consequently, difference thresholds may be better suited to identify processes of sensitivity control than to derive the spectral sensitivity of color mechanisms.

For the purpose of studying adaptation processes, difference thresholds have been measured with a variety of methods. Wright (1935) used flashed monochromatic bipartite fields to study brightness discrimination at levels different from the adapting brightness. Variations on Wright's basic technique have included the use of flicker (Craik, 1938) and increment thresholds (Heinemann, 1961). King-Smith and Webb (1970) and Shevell (1977) modified Stiles' two-color procedure by using flashed instead of steady backgrounds. The use of flashed backgrounds was refined to estimate properties of static and adaptive mechanisms by Geisler (1978), Hood *et al.* (1978, 1979), Finkelstein and Hood (1981), Adelson (1982) and Hayhoe *et al.* (1987).

The experiments in the present study were designed to measure the range of the differential sensitivity of the $S$-cone system in different states of steady adaptation, and the shift in the range from one adaptation state to another. A novel aspect of these experiments was that spatial and temporal procedures similar to those listed above were used in conjunction with stimuli that varied along theoretically defined lines in color space. To psychophysically isolate the $S$-cone system, the

procedure involved measurements of discrimination thresholds between lights that differed in $S$-cone excitation but not in $L$- or $M$-cone excitation. Lights along different color lines were used to manipulate the adaptation state of the $S$-cone system while maintaining constant adaptation of other color systems, to stimulate different components of the $S$-cone system, and to localize static and adaptive mechanisms in the pre- or post-opponent stages. The color lines were defined on the basis of (1) empirical estimates of the spectral sensitivities of the first stage mechanisms (Smith & Pokorny, 1975) derived from color matches of trichromats and dichromats (Maxwell, 1860; Konig & Dieterici, 1983); and (2) the rules of second stage signal combination identified psychophysically through the selective desensitizing effect of prolonged temporal modulation (Krauskopf *et al.*, 1982). Extended justification for using these particular estimates is given in Zaidi (1992).

## EXPERIMENTAL STRATEGY AND LOGISTICS

### *Skeletal model of the S-cone system*

The skeletal model of the initial stages of the $S$-cone system shown in Fig. 1 was used as a guide in this investigation. In this model, light is absorbed by three types of linear transducers, the $S$-, $M$- and $L$-cones. The spectral sensitivities of these cones are assumed to correspond to the Smith and Pokorny (1975) fundamentals. The outputs of the $L$- and $M$-cones are summed into an $LM$ signal. The difference between the $S$-cone and $LM$ signals constitutes an opponent chromatic signal ($C$). If the outputs of $L$ and $M$ are added in the proportion that gives $LM$ the same spectral curve as $V_\lambda$ (the CIE spectral luminosity function), and if $S$ and $LM$ are combined so that $C$ is equal to zero when the incident light is an equal-energy white, then the system in Fig. 1 will possess the spectral properties of the $S$-cone cardinal mechanism of Krauskopf *et al.* (1982). This is because it will respond to modulation in the exclusive $S$-cone direction but not in the other cardinal directions. In this study, assumptions about the combination at $C$ were tested by manipulating the $S$ and $LM$ signals in an independent fashion.

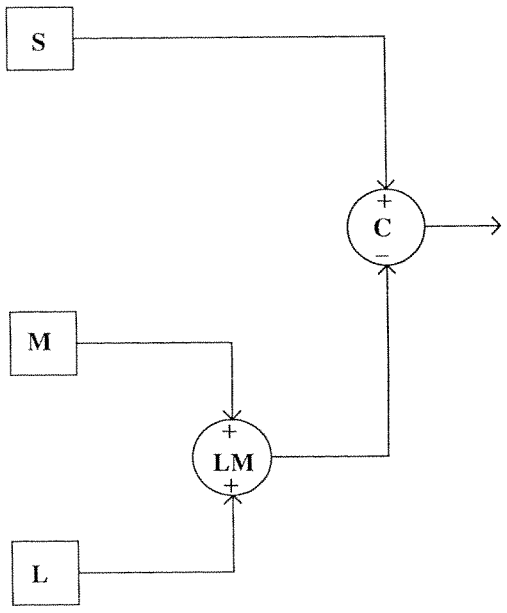


FIGURE 1. The skeletal model of the initial stages of the $S$-cone system used as a guide for the experiments in this paper. The $S$-, $M$-, and $L$-cones act as three types of linear transducers. The signals from the $L$- and $M$-cones are summed to make the $LM$ signal. The difference between the $S$ and $LM$ signals constitutes an opponent chromatic signal ($C$).

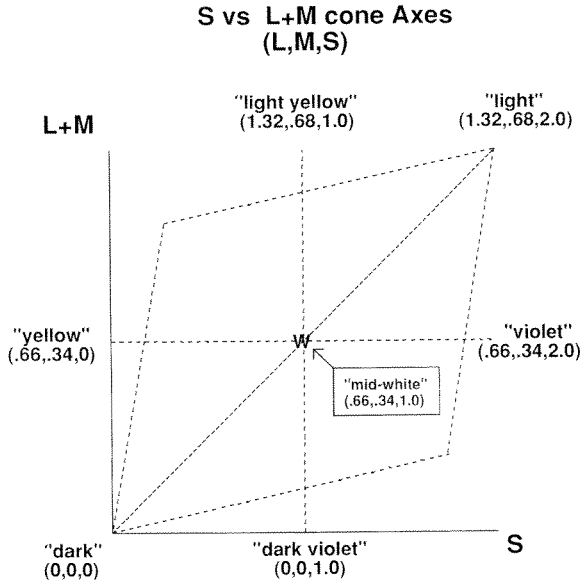


FIGURE 2. Schematic of the color plane defined by the $S$ and $L + M$ color axes. The ordered triplets ($L$, $M$, $S$) were obtained by transforming the CIE (1931) coordinates for each light to Smith–Pokorny (1975) fundamentals. The light at W is metameric to equal-energy white with a luminance defined to be 1 unit. The heights of the cone fundamentals at W were adjusted so that $L + M = V_\lambda$ (the CIE spectral luminosity function) and $S = L + M = 1$. The excitations for each cone type change in a linear fashion along every straight line in the plane. Lights along horizontal lines differ solely in $S$-cone excitation. Lights along vertical lines differ in the sum of the $L$ and $M$ excitations. The diagonal line labeled "light–dark" represents achromatic colors varying linearly in luminance. The quadrilateral boundary encloses lights that could be generated by the equipment.

### *The S vs L + M color plane*

The $S$-cone system has been extensively studied with a variety of methods (see Pugh & Mollon, 1979; Pokorny *et al.*, 1981; Williams, MacLeod & Hayhoe, 1981; Mollon, 1982; Stockman *et al.*, 1991; for references). In the present investigation, the properties of the $S$-cone system were examined in a particularly direct manner, by manipulating lights to selectively stimulate different components of the $S$-cone system. These manipulations were made possible by the stimulus generation capabilities of color television monitors and computer frame-buffer generators. The lights were restricted to one plane of a three-dimensional color space: the plane defined by the $S$ and $L + M$ axes shown in Fig. 2. Lights are represented in the figure by ($L$, $M$, $S$) cone excitations that were obtained by transforming the CIE (1931) co-ordinates for each light to Smith–Pokorny (1975) fundamentals. The heights of the cone fundamentals were set so that $L + M$ was equal to $V_\lambda$, and $S$ was equal

to $L + M$ for an equal-energy white. In this representation, cone excitations change in a linear fashion along every straight line in the figure. At unit luminance, the $L$ and $M$ units in Fig. 2 are equal to the "r" and "g" units respectively of the MacLeod and Boynton (1978) chromaticity diagram. The light at W, the center point, is metameric to equal-energy white with a luminance defined to be 1 unit. The ratio of $L$ to $M$ at W is 2:1 and the sum $L + M$ is equal to unity. One $S$ unit is equal to one "b" unit of MacLeod and Boynton multiplied by a constant to make $S$ equal to 1 at W.

The diagonal line labeled "light–dark" represents achromatic colors varying linearly in luminance. At the "dark" point, $S = M = L = 0$, due to the absence of light. At the "light" point, the excitation of each cone type is twice that at W. The scale along the "light–dark" line is a linear scale, where the excitation of each cone type is proportional to the luminance of the incident light. Lights along horizontal lines differ solely in $S$-cone excitation. Because there are no physically real lights that are absorbed exclusively by $S$-cones, there are no lights that correspond to the horizontal axis passing through the "dark" point. However, the horizontal line passing through W consists of real lights that are equiluminant tritanopic confusion pairs with W, and represents a linear scale for pure $S$-cone changes. If the horizontal line through W is extended to the left, it cuts the spectrum locus at around 570 nm ("yellow") where $S$ is equal to zero. Since $S$ is equal to one at W and zero at the "dark" and "yellow" points, the "light–dark" and "yellow–blue" axes can be related to each other in terms of $S$-cone excitation. The "violet" end of the horizontal line is the point where $S$ is twice the value it is at W. Once the two linear scales described above have been set, $L + M$ is equal to zero at the "dark" point and one at "yellow" and W, enabling a comparison of the "light–dark" and vertical axes in terms of $L + M$ excitation.

The color names in Fig. 2 reflect the approximate appearance of lights and are meant to be used only as mnemonic aids. The colors displayed on the screen were more desaturated than the names suggest. The region enclosed by the dashed quadrilateral boundary includes all the colors in this color plane that could be generated with the equipment used in this study. The complete set of visible lights in this color plane stretches past these limits in the rightward and upward directions.

The units for $L$, $M$ and $S$ in Fig. 2 were chosen so that when all the combination weights in Fig. 1 were unity, the system satisfied the properties of the $S$-cone cardinal mechanism. Using W as the center of reference, illuminant changes on the color plane can be related to responses of different parts of the skeletal $S$-cone system. At W, since $S = L + M$, the opponent signal $C$ is equal to zero. A change in color from W along the horizontal axis, will be registered by the $S$ branch but not the $LM$ branch, and a change parallel to the vertical axis by the $LM$ branch but not the $S$ branch.

*Design of experimental conditions*

To distinguish between sensitivity limitations due to static processes and sensitivity changes due to adaptive processes, a variant of the probe-flash technique (Hood *et al.*, 1978) was used. The lights used in these experiments were divided into three classes: adapting lights, flashes and probes. Adapting lights were constantly present for the duration of a particular condition. Once an observer was adapted to a steady light, sensitivity at that color was estimated by the difference threshold for a brief change in the relevant color direction. The light to be discriminated from the adapting light was termed a probe. The probe was spatially smaller than the adapting light and was on for a period considered too short to disturb the state of adaptation. This steady state procedure, however, estimated sensitivity only at the adaptation color. To estimate differential sensitivity over a larger range the observer made difference judgments at points in color space other than the adapting color. A light different from the adapting light was flashed simultaneously with the probe, and the observer was required to spatially discriminate the probe from the flash. Discrimination between the probe and the flash was only possible during a period too brief to alter the adaptation state of the observer significantly. This procedure was repeated for different adapting lights to estimate the change in sensitivity due to adaptive processes. The point in color space that represents the superimposition of the adapting and flashed lights will be referred to as the "judgment" point or color.

In the $S$-cone system depicted in Fig. 1, differential sensitivity could be limited due to the response limitations of static mechanisms located before or after the opponent combination of cone signals. Similarly, adaptive processes could occur before or after the opponent combination. Static and adaptive processes were localized by choosing lights from three axes on the color plane in Fig. 2 for the adapting background, flash and probe. Steady adapting lights of different colors along the horizontal axis differ in their effects on the adaptation state of $S$-cones and the subsequent mechanisms that process $S$-cone signals, whereas adaptation states of the mechanisms that do not process $S$-cone signals remain constant. In addition, within the $S$-cone system, only pre-opponent adaptive mechanisms on the $S$ branch and post-opponent adaptive mechanisms could be involved in changes in sensitivity, not pre-opponent mechanisms on the $LM$ branch. Adapting lights along the vertical axis differ in their effects on the state of mechanisms that respond to change in the sum of $L$ and $M$ excitation. For the $S$-cone system, these include mechanisms on the pre-opponent $LM$ branch and post-opponent mechanisms. Interpreting a change of adaptation along the "light–dark" line is dependent on the assumed weights of cone–signal combination; in Fig. 2, the opponent signal equal to $S-(L + M)$ is equal to zero all along the diagonal axis, so that any adaptive changes have to be due to pre-opponent mechanisms. In any state of adaptation, the response of static mechanisms in different parts of the $S$-cone system was examined by using flashes that differed from the adapting field in a direction parallel to one of the three lines

described above. In all conditions, the observer's discrimination was limited to the $S$-cone system by using a probe that differed from the flash only in $S$-cone excitation, i.e. by keeping the vector difference between the probe and flash parallel to the horizontal axis.

*Methods and procedure*

*Equipment.* Stimuli were displayed on the screen of a Tektronix 690SR color television monitor. The screen was refreshed at 120 interlaced frames per sec. Images were generated using an Adage 3000 raster based frame buffer generator. The Adage allowed for 10 bit specification of the output of each TV gun leading to a palette of $2^{30}$ possible colors of which 256 could be displayed on any frame. All stimulus generation and data collection was done automatically under computer control.

*Calibration.* To specify the chromaticity and luminance of the television output precisely, the system was calibrated as follows: all three guns (R, G, B) were set at the maximum output available from the Adage, and hardware controls on the Tektronix were manipulated to achieve a color approximately metameric to an equal-energy white of 99 cd/m$^2$ (R = 24.2, G = 64.0, B = 10.8 cd/m$^2$). The setting of this color was determined by using the manufacturer supplied CIE chromaticities of the three phosphors and calculating the luminance of each phosphor needed to give a combined output metameric to equal-energy white. The hardware controls were then locked. For each gun, the luminance of the screen was measured with a UDT photometer at each of the 1024 possible output values during 10,000 up and down series. For each gun the luminance of the screen was a non-linear function of the input voltage. The stored average values were used to compute back-transform tables to enable linear specification of the output of the guns.

The fractional luminances of the three phosphors $B_I$, $G_I$, $R_I$ were defined as the ratios of the luminances at $I$ to the maximum luminances for the $B$, $G$ and $R$ phosphors, respectively.

Points along the "light–dark" line in Fig. 2 correspond to equal output values of the three guns. The "dark" point corresponds to $R_d = G_d = B_d = 0$, and the "light" point to $R_l = G_l = B_l = 1.0$. The W point corresponds to the achromatic color of the screen when all three guns were set at the mid-point of their range, i.e. $R_w = G_w = B_w = 0.5$. One unit of luminance in this paper was specified as equal to 49.5 cd/m$^2$, which was equal to the luminance of the horizontal axis in Fig. 2.

The horizontal axis in Fig. 2 consists of lights that vary from W only in $S$-cone excitation, i.e. the $L$- and $M$-cone excitation is identical for all lights along this axis. The $R$, $G$, $B$ values for these lights were determined by first converting the chromaticity of the phosphors to cone excitations in the units used in Fig. 2. The $S$, $M$ and $L$ values at the maximum output of the three phosphors $R$, $G$ and $B$ were as follows:

$$(S_B, M_B, L_B) = (1.687, 0.104, 0.114)$$

$$(S_G, M_G, L_G) = (0.237, 0.498, 0.795)$$

$$(S_R, M_R, L_R) = (0.030, 0.084, 0.405).$$

The cone excitations $L_I$, $M_I$ and $S_I$ for light $I$ were calculated by using the $S$, $M$ and $L$ values of the phosphors with their fractional luminances at $I$:

$$L_I = B_I L_B + G_I L_G + R_I I_R$$

$$M_I = B_I M_B + G_I M_G + R_I M_R$$

$$S_I = B_I S_B + G_I S_G + R_I S_R.$$

For any color H on the horizontal axis, different from W, $S_H$ is not equal to $S_W$ but $L_H$ is equal to $L_W$, therefore:

$$(B_W - B_H) - L_B = (G_H - G_W) L_G + (R_H - R_W W) L_R.$$

Moreover, $M_H$ is equal to $M_W$, therefore:

$$(B_W - B_H) M_B = (G_H - G_W) M_G + (R_H - R_W) M_R.$$

The only unknowns in these two simultaneous equations are $R_H$, $G_H$ and $B_H$. The full range of displayable colors on the horizontal axis is found by solving these equations for $G_H$ and $R_H$ as $B_H$ is varied from 0 to 1.

$R$, $G$ and $B$ gun values for the vertical $L + M$ axis were determined by taking vector differences between the "light–dark" and "yellow–blue" axes. For example, moving up from W on the "light–dark" axis increases $L$, $M$ and $S$ excitations. By then moving left parallel to the horizontal axis, $S$ excitation alone is reduced and a point V is reached on the vertical axis, where $S_V$ is equal to $S_W$, but $L_V$ and $M_V$ are greater than $L_W$ and $M_W$.

*Procedure.* The spatial configuration and the temporal sequence of stimuli are shown in Fig. 3. The adapting and flashed fields were spatially identical 10° squares. The probe consisted of two quadrants of a 3° disk concentric with the flash. This butterfly shape was chosen over the usual circular probe for two reasons: (i) with a circular probe, discrimination from the flash takes place on the outer edge of the probe, while with the butterfly shape, the center of the fovea can be used for discrimination; (ii) the flashes used in this experiment often made a roughly circular Maxwell's spot transiently visible, which would have interfered with judgments about the presence or absence of a circular probe.

At the beginning of the experiment the observer fixated on the center of the adapting field for 120 sec. Following three warning beeps, the flash and the probe were presented simultaneously. After 0.05 sec the probe was turned off, but the flash stayed on for an additional 0.45 sec. Previous work with the probe-flash technique had shown that unless the probe was shorter than the flash, discrimination could be based on different persistences of the probe and flash signals (Geisler, 1979). The 0.05 sec duration for the probe was a compromise between keeping the probe as short as possible so as not to disturb adaptation, and making it long enough to measure thresholds for a variety of conditions within the range of the equipment. Before each probe-flash presentation the observer was exposed to the initial adapting field for 10 sec.

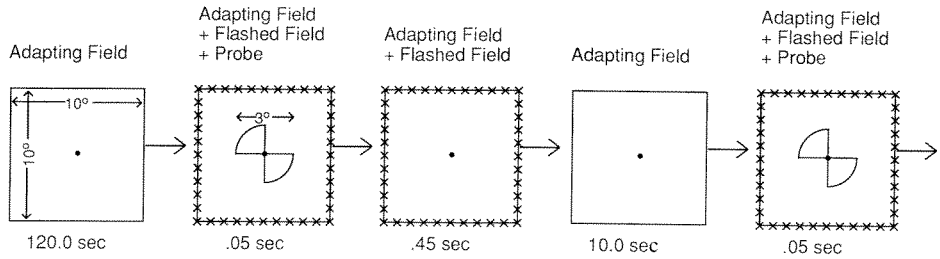


FIGURE 3. The spatial configuration and the temporal sequence of the stimuli. The adapting field (solid outlines) and flashed field (crossed outlines) were spatially identical 10° squares, and the probe was two quadrants of a 3 deg disk. At the beginning of the experiment the observer fixated at the center of the adapting field for 120 sec. The 0.05 sec probe was present at the onset of the 0.05 sec flash. The inter-trial interval was 10 sec.

The observer pressed buttons to indicate if the probe could be discriminated from the surround. A double random staircase was run for each condition, tracking the 70% point on the psychometric curve. Each data point was the mean of 12 reversals. The standard error of the measurements was generally around 10% of the mean value. In each experimental session the state of adaptation was kept constant, and staircases for a number of flash conditions were randomly interleaved. The experiment was run in a darkened room. The observer viewed the screen binocularly through natural pupils. The distance between the screen and the observer was kept constant at 6 ft by means of a fixed chin and forehead rest.

*Observers.* Two of the authors, AS and QZ, served as observers. Both observers are normal trichromats as measured by standard color-vision tests, and have normal visual acuity.

## EXPERIMENT 1

In the first experiment, adaptive processes in the $S$-cone system were localized by measuring difference thresholds at steady adapting lights distributed along the $S$ and $L + M$ axes and the "light–dark" line (Fig. 4). These thresholds were termed steady-state thresholds, and are plotted vs the adapting lights in Fig. 5(a) (b) and (c). In this paper, lights are described in units that are unfamiliar to many readers, so with each set of data, a schematic panel is included that locates adapting lights (and flashes where pertinent) on $S$ vs $L + M$ color diagrams. In addition, the effect of these lights on the $S$-cone system is depicted on skeletal diagrams similar to Fig. 1.

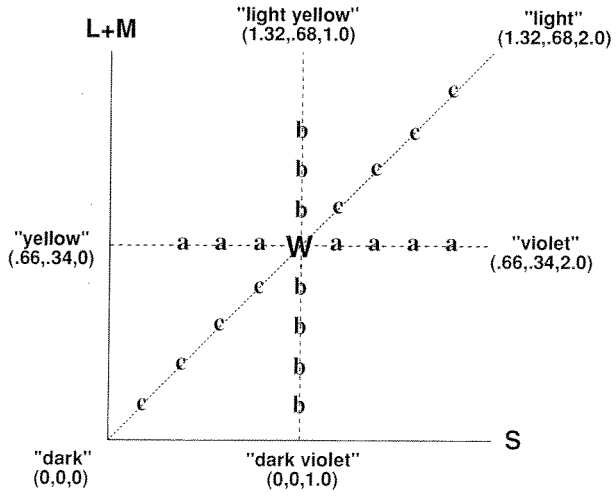


FIGURE 4. Adaptation conditions for Expt 1. The letters, "a", "b", and "c" represent the sets of adapting lights for the steady-state (no flash) conditions. Thresholds for $S$-cone decrements were measured at each of these points.

In Fig. 4, the points labeled "a" represent a set of adapting lights on the $S$ axis through W. Shifting adaptation from one "a" to another changed the state of only those color systems that are driven by the $S$-cones. In terms of the skeletal $S$-cone diagram in Fig. 5(a), the change in adaptation leads to changes along the $S$ branch, or subsequent to the opponent combination, but not along the $L + M$ branch. The adaptation lights used for the data in Fig. 5(a) correspond to "a"s in Fig. 4. The horizontal axis is scaled in the same $S$-cone units as Fig. 4. The probes were pure $S$-cone decrements from the adapting lights, i.e. a probe differed from the adapting light by a horizontal vector pointing towards "yellow". Difference thresholds for the probes are plotted in negative $\Delta S$ cone units on the vertical axis. The solid curve is the prediction from a model to be discussed in a later section. The main result in Fig. 5(a) is that as the $S$-cone excitation from the adapting background increased, the difference in $S$-cone excitation between the probe and the background required for discrimination also increased. This could be due to changes in the $S$-cone system either before or after the opponent combination. The data seem to have two limbs, a shallow one to the left of W where $S < 1.0$ and a steeper one to the right where $S > 1.0$.

Thresholds for $S$-cone decrements from a number of adapting lights on the $L + M$ axis through W are shown in Fig. 5(b). The locations of the adapting lights are marked by "b"s on Fig. 4. Since the adapting lights differed only in $L + M$ excitation, difference thresholds are plotted against the adapting $L + M$ value. Increasing only the $L + M$ component of adapting backgrounds seems to have no effect on the thresholds for $S$-cone decrements.

The scales for $S$ and $L + M$ were chosen so that Fig. 5(a) and (b) could be directly compared in terms of the

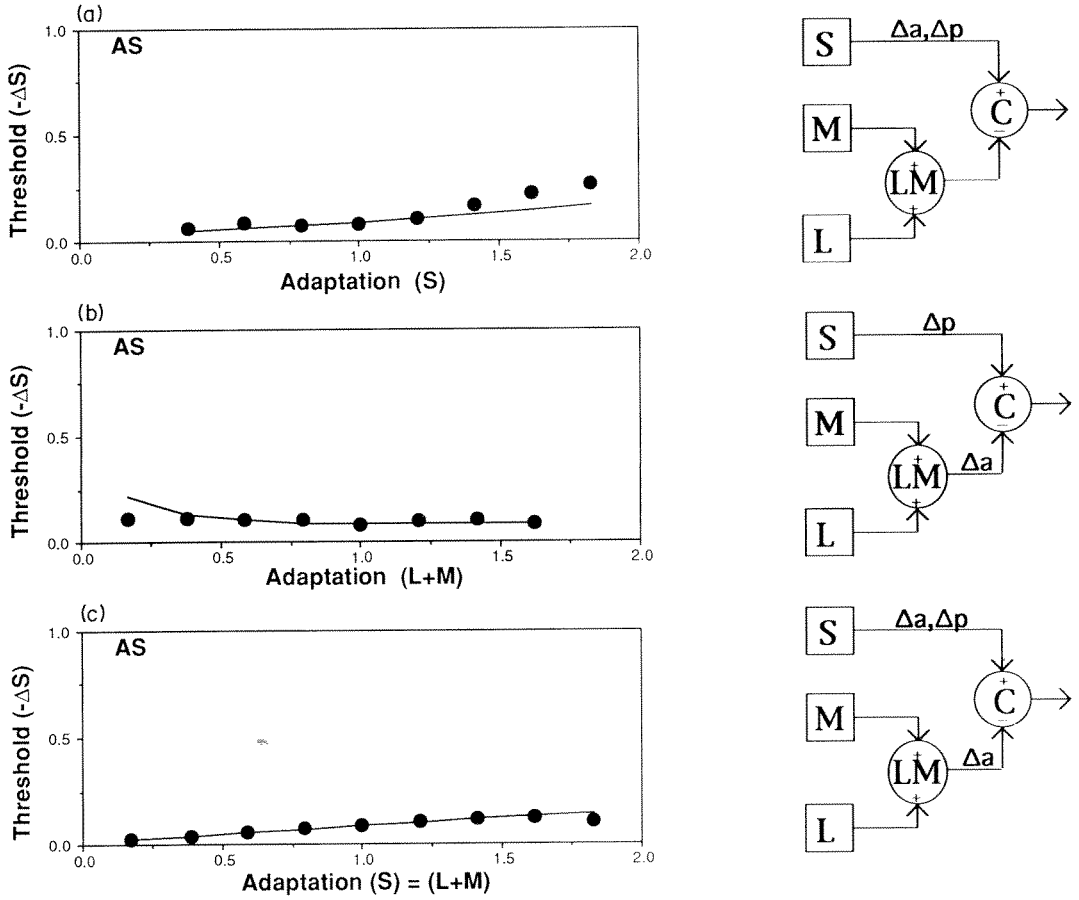


FIGURE 5. Results from Expt 1. The left part of each panel shows the difference thresholds for the steady-state (no flash) conditions plotted vs the adapting light in either $S$ or $LM$ units. The adapting lights in (a) were at different points along the $S$ axis and are represented in Fig. 4 by points labeled "a". In (b), the adapting lights were at different points along the $L+M$ axis and are represented in Fig. 4 by points labeled "b". In (c), the adapting lights were at different points along the "light–dark" diagonal and are represented in Fig. 4 by points labeled "c". The right part of each panel shows the effect of each condition on the $S$-cone system. In each skeletal diagram, "Δa" indicates those branches of the system affected by a change in the adapting light, and "Δp" indicates those branches affected by the probe.

adapting $S-(L+M)$ excitation. Since $L+M$ is equal to 1 for all the adapting lights in Fig. 5(a), subtracting 1 from the horizontal scale gives the $S-(L+M)$ coordinates of the adapting lights, from $-1$ to $+1$. As $S$ excitation was equal to 1 for all the adapting lights in Fig. 5(b), subtracting the horizontal co-ordinate from 1 gives the $S-(L+M)$ coordinate. [$S-(L+M)$ increases towards the right in Fig. 5(a) but towards the left in 5(b).] The results indicate that in contrast to the effect of increasing $S$-cone adaptation levels, the $S$-cone system discounts the effect of different steady levels of $L+M$ excitation on $S$ probes. Post-opponent adaptive processes can affect $S$ probes solely as a function of the steady $S-(L+M)$ level but not of the $S$ or $L+M$ levels individually. Because changes in the steady $L+M$ level can affect sensitivity to $S$ probes only through processes subsequent to the opponent combination (see skeletal diagram), adaptation in the $S$-cone system to different steady levels of $L+M$ must occur at a pre-opponent level so that the state of post-opponent mechanisms is kept fairly constant.

For steady adapting lights along the "light–dark" diagonal (shown as "c"s in Fig. 4), $S$, $L$ and $M$ excitations change in a proportional manner such that the opponent signal $S-(L+M)$ is always zero. Thresholds for $S$-cone decrements on these backgrounds are shown in Fig. 5(c). The adapting lights are plotted in $S$-cone units on the same scale as Fig. 5(a). Since these adapting lights differ in $S+L+M$, multiplying the horizontal axis by 2 gives the $S+L+M$ coordinate. For observer AS, $S$-cone discrimination thresholds increase approximately linearly with an increase in $S+L+M$. Since $S-(L+M)$ is zero for all these adapting lights, the threshold changes are due to changes in the pre-opponent $S$ branch only. The slope of the straight line fitted to the data in Fig. 5(c) is equal to 0.075, not appreciably different from 0.087, the Weber fraction for $\Pi_1$ (Stiles, 1959).

The difference between the results in Fig. 5(a) and (c) shows that the steady excitation level of the $S$-cones is not the sole determiner of the thresholds in Fig. 5(a), and post-opponent mechanisms are partly responsible. The difference between the results in Fig. 5(a) and (b) indicates that adaptive processes in the $S$-cone system mainly occur independently in the two pre-opponent branches.

## EXPERIMENT 2

In the second experiment, static mechanisms that limit sensitivity in the $S$-cone system were localized by measuring discrimination thresholds at judgment points on two color lines passing through the adapting point. By using flashed fields, the state of adaptation was kept constant. In the first part of this experiment, the flashes were pure $S$-cone increments or decrements from the steady W adapting field, and the probes were pure $S$-cone decrements from the flashes [see skeletal diagram in Fig. 6(a)]. In the color diagram in Fig. 6(b), the adapting field is at W and the colors of the flashes are represented by asterisks. Difference thresholds are plotted in negative $\Delta S$ cone units as solid circles in Fig. 6(c). Flashes are expressed as $S$-cone increments or decrements from the steady background. The threshold for the flash with a value of zero corresponds to a difference threshold on the steady adapting background. The most noticeable pattern in the data is the V-shape. Discrimination is best at the steady W background. As the $S$-cone difference between the flash and the steady background increased on either side, increasingly larger $S$-cone differences between probe and flash were required for discrimination. The open squares on this figure are data from Fig. 5(a) and represent probe thresholds measured against steady fields of identical color as the flashed judgment points. A comparison of the solid circles and open squares shows that adapting to a steady field improves discrimination around that color. As $\Delta(L + M)$ is zero for these flashes, the numbers on the horizontal axis also represent the flashes expressed in terms of increments and decrements in the opponent signal $\Delta[S - (L + M)]$. The results for the second observer, plotted in Fig. 6(d), show a pattern similar to the first observer's.

In the second part of the experiment, the flashes were $L + M$ increments or decrements from the steady W adapting field, and the probes were again pure $S$ decrements from the flashes [see skeletal diagram in Fig. 7(a)]

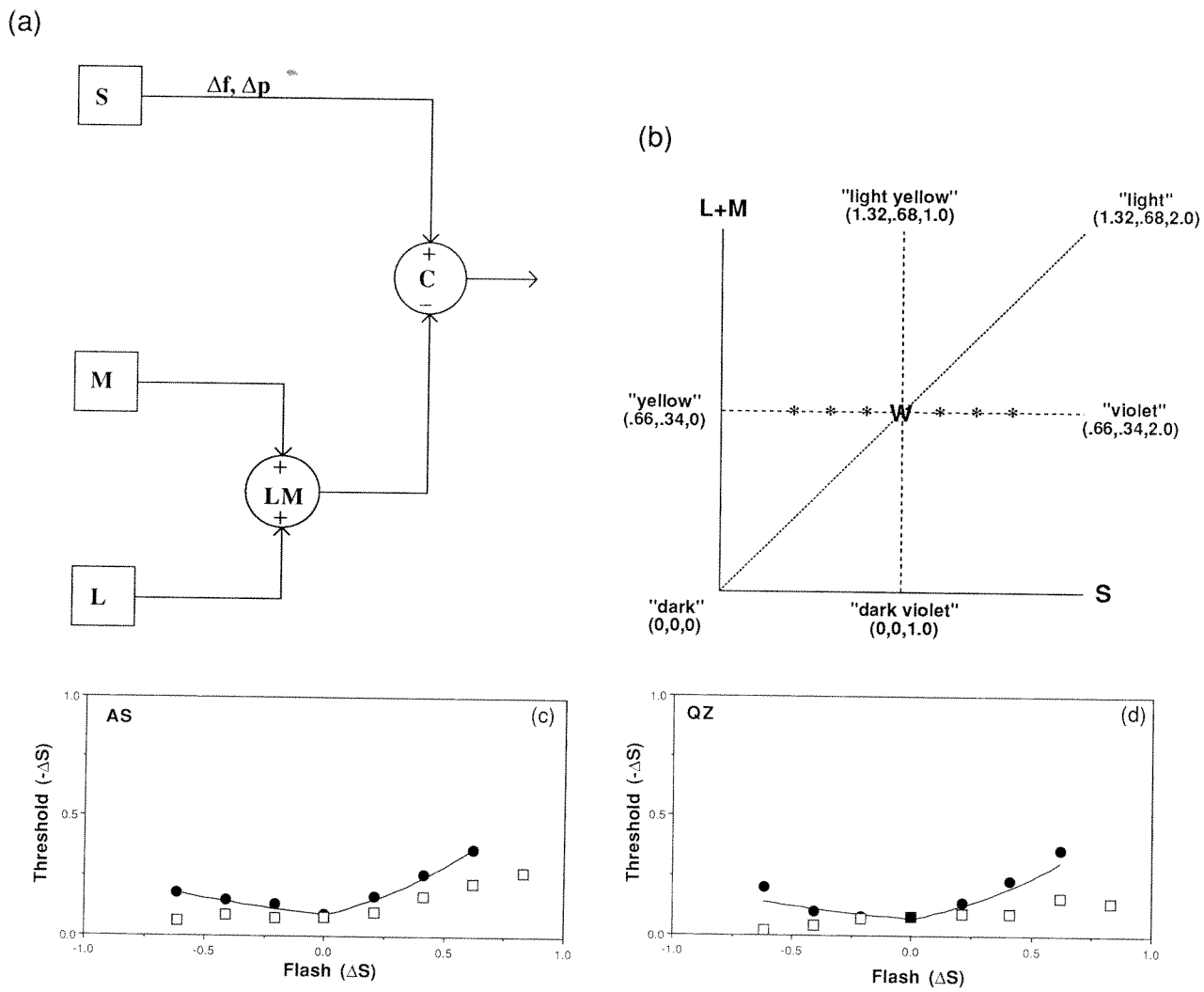


FIGURE 6. (a) The effects of the lights in the first part of Expt 2 on a skeletal model of the $S$-cone system. Δf identifies those branches of the system affected by the flashed fields, and Δp identifies those branches affected by the probe. (b) The stimulus conditions in the color plane for the first part of Expt 2. Thresholds were measured for $S$-cone decrements at different judgment points on the $S$-cone axis following adaptation to W. The asterisks represent the flashed fields that were used as judgment points. (c) The solid circles are the difference thresholds shown as a function of the judgment point's $S$-cone increment or decrement from the adapting field. For comparison the squares are the difference thresholds for the same judgment points presented as steady fields replotted from Fig. 5(a). (d) The same comparison for observer QZ.

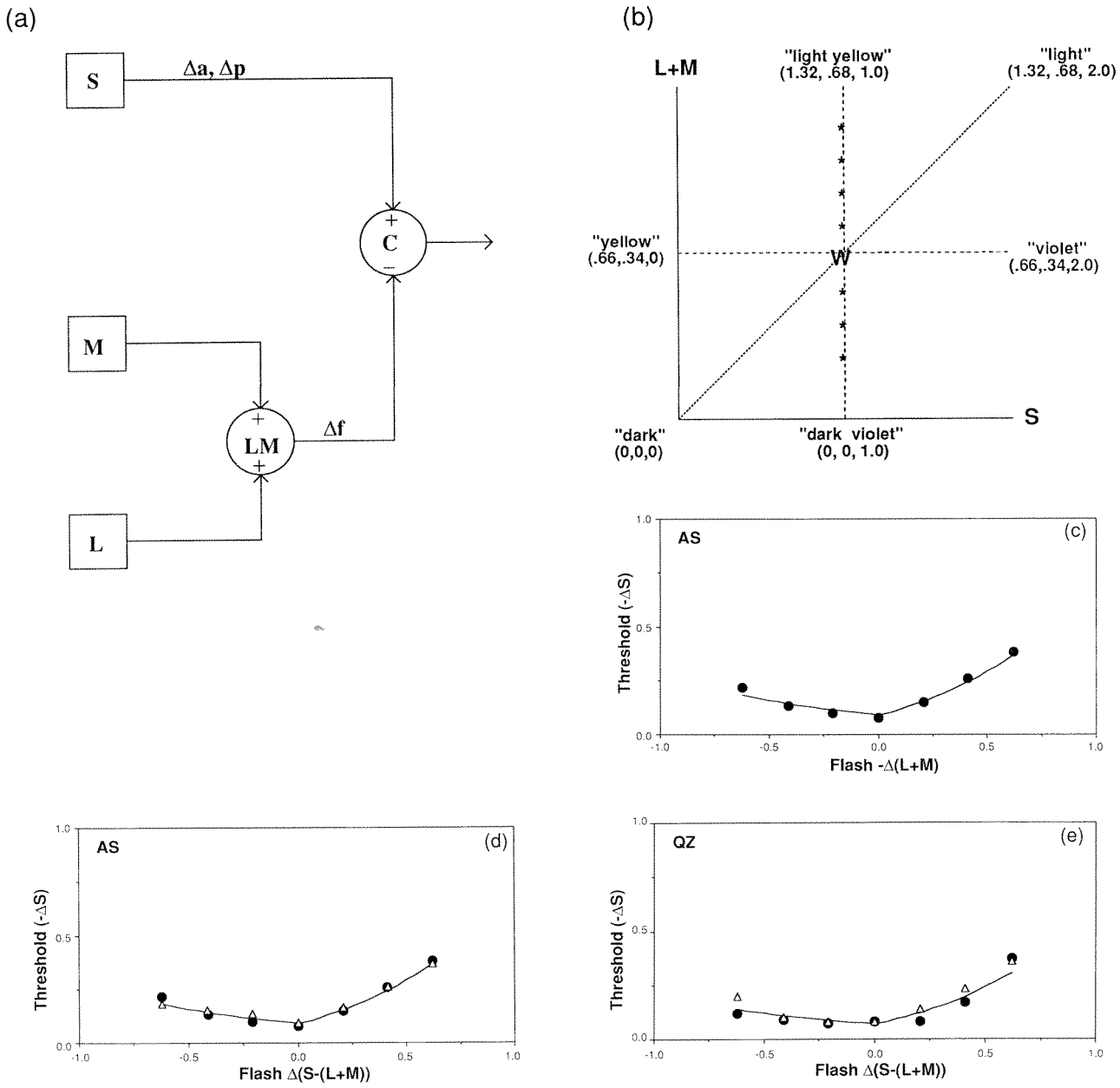


FIGURE 7. (a) The effects of the lights in the second part of Expt 2 on a skeletal model of the $S$-cone system. Δa identifies those branches affected by changes in the adapting field, Δf the flashed field and Δp the probe. (b) The stimulus conditions in the color plane for the second part of Expt 2. Thresholds were measured for $S$-cone decrements at different judgment points on the $L + M$ axis following adaptation to W. The asterisks represent the flashed fields that were used as judgment points. (c) The solid circles are the difference thresholds shown as a function of the judgment point's $L + M$ increment or decrement from the adapting field. (d) The solid circles are the data from (c) replotted in $\Delta[S\text{-}(L + M)]$ units. For comparison the triangles are the difference thresholds for the $\Delta S$ flashes replotted in $\Delta[S - (L + M)]$ units. (e) The same comparison for observer QZ.

In the color diagram in Fig. 7(b), the adapting field is at W and the colors of the flashes are represented by asterisks. Difference thresholds are plotted in negative $\Delta S$ units as solid circles in Fig. 7(c). Flashes are expressed as negative $L + M$ increments or decrements from W. The most noticeable pattern is the V shape, i.e. sensitivity decreases with increasing distance from the adapting color in both positive and negative $L + M$ directions. Since $\Delta S$ was zero for these flashes, the change from the adapting light in $\Delta[S - (L + M)]$ units was also equal to the value shown on the horizontal scale.

Probe discrimination from the $S$-cone flashes in Fig. 6(c) can be compared to discrimination from $L + M$ flashes in Fig. 7(c), by expressing both sets of flashes in equivalent $\Delta[S - (L + M)]$ units. In Fig. 7(d), the data from Fig. 6(c) is replotted as open triangles and the data from Fig. 7(c) as solid circles. The open triangles coincide with the solid circles, showing that when the observer was adapted to W, thresholds were a function of the $S - (L + M)$ difference between the flash and W regardless of whether the difference was along the $S$ or the $L + M$ directions. Since the $L + M$ flashes can only affect sensitivity to $S$ probes after the opponent

combination, these results indicate that the main static response limitation is located posterior to the opponent combination of $S$ and $L+M$ signals. In addition, the similarity of the two threshold curves indicates that in the excitation units used in Fig. 2, the $S$ and $L+M$ signals are weighted equally but with opposite signs at the combination stage C. The results for the second observer, plotted in Fig. 7(e), show a pattern similar to the first observer's.

## MODEL

The model of the $S$-cone system shown in Fig. 8 consists of the skeletal system with adaptive and static mechanisms added on the basis of the results of Expts 1 and 2. Like the skeletal model, the first stage consists of the $S$ and $LM$ $(=L+M)$ linear transducers of light energy. The results of Expt 1 indicate that adaptive processes adjust the response of the $S$-cone system mainly before the opponent combination of signals from the $S$ and $LM$ branches. In the model, this is accomplished by multiplying the signal in each pre-opponent branch by a scalar that represents the gain of the adaptive mechanism. The gain in each branch depends only on the steady signal in that branch and is calculated according to the decreasing function shown in the boxes. Because the results of Expt 2 indicate that the $S$ and $LM$ signals have equal but opposite weights at the opponent combination, $C$ is simply set equal to $S-(L+M)$. The results in Fig. 7(d) shows a loss of differential sensitivity on both sides of the adapting light W as a function of $\Delta[S-(L+M)]$. In the model this is attributed to a post-opponent static mechanism whose response is a sigmoidal function of the opponent input, i.e. a diminishing differential response to unit input differences on both sides of zero. Since both difference threshold curves in Fig. 7(d) are steeper on the positive side of $\Delta[S-(L+M)]$, the response curve is more compressed on that side. The response of the static mechanism is transmitted to higher levels and two lights can be discriminated by an observer only if the difference in response to the lights is greater than a constant limen. In the remainder of this section, the mathematical specification of the model and its quantitative estimation will be described in detail. In the succeeding sections, the model will be tested in a variety of situations.

In Fig. 8, $S$ has the spectral sensitivity of $S$-cones and $LM$ the spectral sensitivity of $V_\lambda$. The $S$ signal at any instant is multiplied by a scalar $\kappa_S$ whose value is a monotonically decreasing function of $S_a$, the response of the $S$-cones to the steady adapting light a. The gain of the adaptive mechanism in the $S$ branch is equal to $\kappa_S$. In a more general model the gain would be a function of the weighted mean of the history of light exposure, so that the gain would change slowly in response to a sudden change of the incident light. In this study, the observer was exposed to a steady adapting light for a prolonged period before every measurement, so the gain was assumed to be a function of the adapting light alone. The form of the function chosen for analytic purposes was:

$$\kappa_S = \frac{\kappa}{\kappa + S_a}. \tag{1}$$

The value of $\kappa_S$ is equal to 1 when $S_a$ is equal to 0 and declines monotonically as $S_a$ increases. The rate of decline is governed by the free-parameter $\kappa$ to be estimated from the data. Similarly the $LM$ signal is multiplied by $\kappa_{LM}$ whose value is a function of $LM_a$:

$$\kappa_{LM} = \frac{\kappa}{\kappa + LM_a}. \tag{2}$$

The value of $\kappa$ is assumed to be the same in equations (1) and (2). The general shape of these functions is shown in Fig. 8, where $\kappa_S$ is plotted vs $S_a$ and $\kappa_{LM}$ vs $LM_a$.

The signal "$\kappa_{LM}LM$" is then subtracted from "$\kappa_S S$" to give an opponent signal $C$. The response of the opponent-stage, $R$, is a sigmoidal function of $C$ given by equations (3) and (4):

If $C>0$

$$R = \rho_\phi(1-e^{-\phi C}) \tag{3}$$

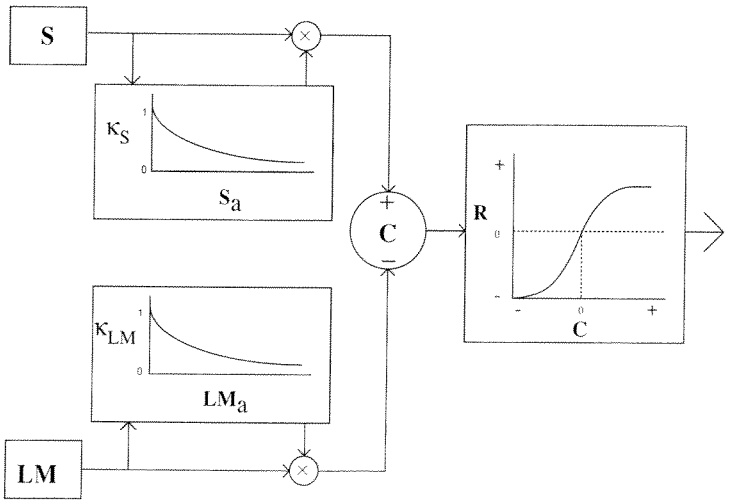


FIGURE 8. A model of the $S$-cone system with adaptive and static mechanisms. Like the skeletal model in Fig. 1, the opponent signal is the difference between the $S$ signal and the sum of the $L$ and $M$ signals. Based on the results of Expt 1, multiplicative gain controls have been added to the $S$ and $LM$ branches before the opponent site. Based on the results of Expt 2, a compressive non-linearity has been added following the opponent site.

else if $C \leqslant 0$

$$R = -\rho_v(1 - e^{vC}). \quad (4)$$

where $\rho_\phi$, $\rho_v$, $\phi$ and $v$ are free parameters to be estimated from the data. The value of $R$ is equal to zero when $C$ is zero, otherwise $R$ has the same sign as $C$. The general shape of $R$ vs $C$ is shown in Fig. 8. The parameters $\phi$ and $v$ govern the curvature of the response function, and $\rho_\phi$ and $-\rho_v$ are equal to the maximum possible positive and negative responses respectively.

Equations (1)–(4) completely specify the model. The response of the model to the lights used in the experiments in this study was calculated as shown below. The observers task was to discriminate between two lights, one consisting of the superimposition of the adapting, flash and probe lights and the other of the superimposition of just the adapting and flash lights. In the equations below, a, f and $\rho$ will be used as subscripts for the adapting, flash and probe lights respectively. The flashes will be expressed as $S$ and $LM$ increments or decrements from the adapting light, and the probes as $S$ decrements from the flash.

The opponent signal from a steady adapting field is given by:

$$C_a = \kappa_S S_a - \kappa_{LM} LM_a. \quad (5)$$

The opponent signal from a flash superimposed with an adapting light is equal to:

$$C_{a+f} = \kappa_S(S_a + S_f) - \kappa_{LM}(LM_a + LM_f). \quad (6)$$

Since the probe was a pure $S$-cone decrement the opponent signal from an adapting light, a flash and an $S$-probe superimposed together is equal to:

$$C_{a+f+p} = \kappa_S(S_a + S_f - S_p) - \kappa_{LM}(LM_a + LM_f). \quad (7)$$

The response of the system was linked to measurements of difference thresholds by the psychophysical assumption that two lights could be reliably discriminated at threshold if the difference in response passed to higher stages was equal to 1 unit. So that at threshold:

$$R_{a+f} - R_{a+f+p} = 1. \quad (8)$$

One consequence of equations (3), (4) and (8) is that thresholds will be higher when the response to the judgment color falls on the compressive portion of the response curve. The model's prediction for "$S_p$" the value of the probe at threshold can be derived by substituting expressions for the $S$-cone system's responses into equation (8) and solving for $S_p$. Since the model allows for the possibility that $\phi$ is different from $v$ and $\rho_\phi$ from $\rho_v$, three different cases have to be considered separately:

(i) When $C_{a+f} > 0$ and $C_{a+f+p} > 0$, by substituting the response values given by equation (3) into equation (8), at threshold:

$$\rho_\phi(1 - e^{-\phi C_{a+f}}) - \rho_\phi(1 - e^{-\phi C_{a+f+p}}) = 1. \quad (9)$$

Separating $C_{a+f+p}$ into its components, and dividing both sides by $\rho_\phi$:

$$1 - e^{-\phi C_{a+f}} - 1 + (e^{-\phi C_{a+f}})(e^{-\phi C_p}) = \frac{1}{\rho_\phi}. \quad (10)$$

Setting $C_p$ equal to $\kappa_S(-S_p)$ and collecting terms:

$$e^{-\phi\kappa_S(-S_p)} = 1 + \frac{e^{\phi C_{a+f}}}{\rho_\phi}. \quad (11)$$

Taking logs and solving for $S_p$:

$$S_p = \frac{1}{\phi\kappa_S} \ln\left(1 + \frac{e^{\phi C_{a+f}}}{\rho_\phi}\right). \quad (12)$$

(ii) When $C_{a+f} > 0$ and $C_{a+f+p} < 0$, at threshold:

$$p_\phi(1 - e^{-\phi C_{a+f}}) + \rho_v(1 - e^{vC_{a+f+p}}) = 1. \quad (13)$$

Therefore,

$$S_p = -\frac{1}{v\kappa_S} \ln\left(\frac{-1 + \rho_\phi + \rho_v - \rho_\phi e^{-\phi C_{a+f}}}{\rho_v e^{vC_{a+f}}}\right). \quad (14)$$

(iii) When $C_{a+f} <= 0$, at threshold:

$$-\rho_v(1 - e^{vC_{a+f}}) + \rho_v(1 - e^{vC_{a+f+p}}) = 1. \quad (15)$$

Therefore,

$$S_p = \frac{-1}{v\kappa_S} \ln\left(1 - \frac{e^{-vC_{a+f}}}{\rho_v}\right). \quad (16)$$

Equations (12), (14) and (16) can be used to predict probe thresholds for the $S$-cone system, after values for the 5 free parameters: $\kappa$, $\phi$, $v$, $\rho_\phi$ and $\rho_v$ have been estimated. The values of these parameters were estimated from the data shown in Figs 5(c) and 6(c) by the following procedures.

To simplify the estimation, three other terms were defined for steady state thresholds on W. In this condition, $S_a = LM_a = 1.0$, therefore the value of the multiplicative scalar in both branches is $\kappa_{1.0}$:

$$\kappa_{1.0} = \frac{\kappa}{k + 1.0}. \quad (17)$$

On the steady W background, $S_{p_w}$ was defined as the $S$ decrement threshold, and $S_{q_w}$ as the increment threshold. The first step in the estimation procedure was to rewrite $\rho_v$ and $\rho_\phi$ in terms of the empirical estimates of $S_{p_w}$ and $S_{q_w}$. For steady-state thresholds on W, since $S_a = LM_a = 1.0$ and $S_f = LM_f = 0.0$, therefore $C_{a+f} = 0$. Substituting these values into equations (12) and (16) and doing the appropriate algebraic manipulations gives analytic expressions for $\rho_\phi$ and $\rho_v$:

$$\rho_v = \frac{1}{1 - e^{-v\kappa_{1.0}S_{p_w}}} \quad (18)$$

$$\rho_\phi = \frac{1}{e^{\phi\kappa_{1.0}S_{q_w}} - 1}. \quad (19)$$

These expressions will be used to simplify subsequent estimation procedures.

For estimating $\kappa$, the steady-state thresholds measured on different achromatic "light–dark" backgrounds and plotted in Fig. 5(c) were used. For all of these steady

backgrounds, $S_a = LM_a$, therefore $\kappa_S = \kappa_{LM}$ because equations (1) and (2) have the same parameter $\kappa$; moreover $S_f = LM_f = 0.0$, therefore:

$$C_{a+f} = \kappa_S(S_a + S_f) - \kappa_{LM}(LM_a + LM_f) = 0. \quad (20)$$

Substituting this value into equation (16):

$$S_p = -\frac{1}{\nu\kappa_S}\log\left(1 - \frac{1}{\rho_\nu}\right). \quad (21)$$

Substituting equation (18) into equation (21) gives:

$$S_p = \frac{1}{\kappa_S}\kappa_{1.0}S_{p_w}. \quad (22)$$

Using the definitions in equations (1) and (17):

$$S_p = \frac{(\kappa + S_a)\,S_{p_w}}{\kappa + 1.0} = \kappa\left(\frac{S_{p_w}}{\kappa - 1.0}\right) + \left(\frac{S_{p_w}}{\kappa + 1.0}\right)S_a. \quad (23)$$

Therefore, when $S_p$ is plotted vs $S_a$ in Fig. 5(c), the model predicts that the data should fall on a straight line and that $\kappa$ can be estimated by fitting a regression line to the data and using the values of the slope and the intercept:

$$\kappa = \frac{\text{intercept}}{\text{slope}}. \quad (24)$$

The straight line fit to the data in Fig. 5(c) had an $R^2$ of 0.99. For observer AS, $\kappa$ was estimated to be 0.15.

The two exponential parameters, $\phi$ and $\nu$ were estimated using the difference thresholds from pure $S$ flashes during steady adaptation to W that are plotted in Fig. 6(c). For these conditions, $S_a = LM_a = 1.0$ and $LM_f = 0.0$, therefore, when $S_f > 0$, using equation (12) and (19):

$$S_p = \frac{1}{\phi\kappa_{1.0}}\ln[1 + e^{\phi\kappa_{1.0}S_f}(e^{\phi\kappa_{1.0}S_{q_w}} - 1)] \quad (25)$$

and when $S_f < 0$, using equations (16) and (18):

$$S_p = -\frac{1}{\nu\kappa_{1.0}}\ln[1 - e^{-\nu\kappa_{1.0}S_f}(1 - e^{-\nu\kappa_{1.0}S_{p_w}})]. \quad (26)$$

Substituting the estimated value of $\kappa$ and empirical estimates of $S_{p_w}$ and $S_{q_w}$ leaves only $\phi$ and $\nu$ as unknowns. Values for these two parameters were estimated by a nonlinear fit of equation (25) to the positive branch and of equation (26) to the negative branch of Fig. 6(c). For observer AS, the best estimate of $\phi$ was 23 and of $\nu$ was 8. The best fitting curves are shown in Fig. 6(c). Using the estimates of $\kappa$, $\phi$ and $\nu$ for observer AS, $\rho_\phi$ was estimated as 3.2 and $\rho_\nu$ as 11.2 from equations (18) and (19).

With all 5 free parameters estimated from just the data shown in Figs 5(c) and 6(c), and using the specification of light stimuli provided in Fig. 2, the model was used to provide quantitative predictions of $S$ probe difference thresholds for flashes in different color directions in various states of adaptation. These predictions were compared to empirical measurements in Expts 3, 4, 5 and 6 and used to test various components of the model.

## EXPERIMENT 3

In Expt 3, the model was tested by psychophysically isolating the $S$-cone system. This required using stimuli for adapting, flash and probe lights that maintained a constant level of $L$ and $M$ cone excitation. The conditions are schematized in the skeletal model in Fig. 9. The change in the steady adaptation (Δa), the change from the steady background to the flash (Δf), and the difference between the probe and the flash (Δp) were restricted to the pre-opponent $S$ branch and subsequent stages of the $S$-cone system. This was accomplished by measuring the response of the $S$-cone system at different adapting colors along the horizontal axis. When the steady adapting light is changed from W to a different color on the horizontal axis, the only change in the visual system is a change in the excitation level of the $S$-cones and subsequent stages of the $S$-cone system. The locations of the adapting lights are shown by the letters "a–i" on the color diagram in Fig. 10(a). The flashes used in this experiment are shown in the color diagram in Fig. 10(b). For any of the steady backgrounds in Fig. 10(a), a flash consisted of a change to one of the asterisks in Fig. 10(b). The probes were pure $S$ decrements.

Measurements of difference thresholds for observer AS are shown in Fig. 11. Each panel "a–i", corresponds to the state of adaptation designated by that letter in Fig. 10(a). Lights "a–d" were on the "yellow" side and lights "f–i" on the "violet" side of W (point "e"). The horizontal axis shows the flashes in units of $S$-cone changes from the adapting field. The vertical axis shows the magnitude of difference thresholds as $S$-cone decrements from the flash. Difference thresholds in the zero flash condition were measured against the steady adapting field. An important feature of each panel is the point of best discrimination, i.e. the smallest difference threshold. In general, difference thresholds were smallest around the

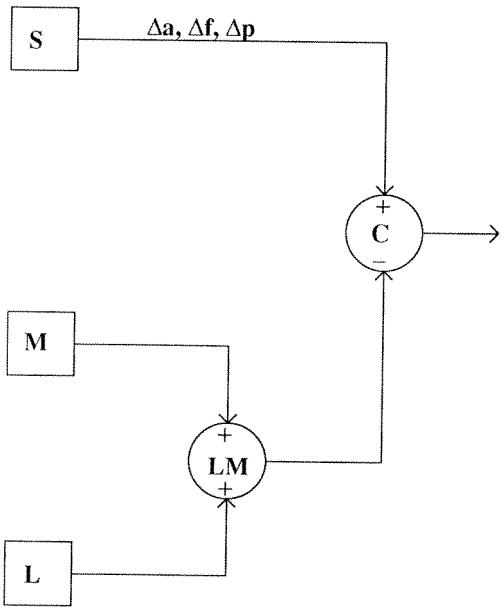


FIGURE 9. The effect of the lights in Expt 3 shown on the skeletal model of the $S$-cone system. "Δa" identifies those branches of the system affected by a change between the steady adapting fields. "Δf" identifies those branches of the system affected by a change from the steady field to the flashed field. "Δp" identifies those branches of the system affected by a change from the flashed field to the probe.

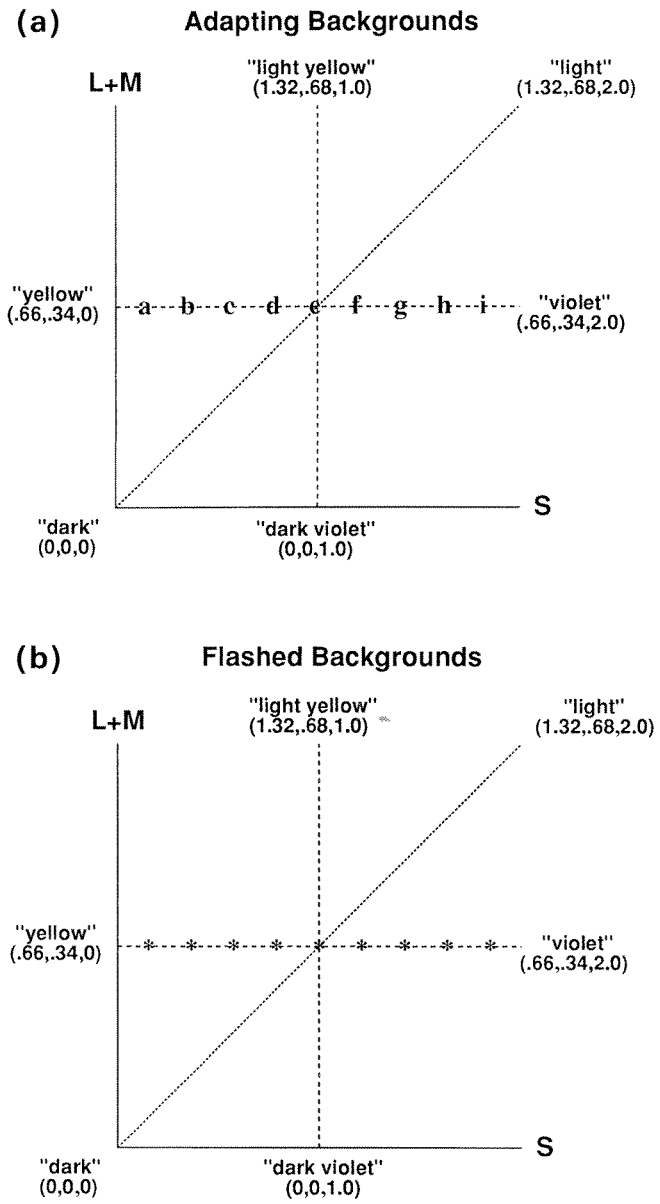


FIGURE 10. Adaptation and flash conditions for Expt 3. In (a) each letter depicts the location of a steady adapting field. In (b), the asterisks represent the location of the flashed fields used as judgment points for each adaptation condition.

adaptation point. However, in the panels on the bottom of the figure, the smallest thresholds are not at the adaptation point, but rather appear shifted toward W from the adapting color. It has not been ascertained whether this is a feature of these experimental conditions or is true even under more prolonged steady adaptation. The solid curves in the figures are predictions from the model based on the quantitative parameters estimated in the last section.

The model reproduces the main features of the data quite well, including the widely different shapes of the threshold curves in different adaptation states. However, the quantitative fit to the data is better for adaptation lights closer to W mainly because the model underestimates steady-state thresholds on the extreme "yellow" and "violet" fields. However, given that a very restricted set of data was used to estimate the parameters and that there were no free parameters in the fits to Fig. 11, the model seems to embody the main processes that govern the sensitivity of the $S$-cone system. The pre-opponent adaptive mechanism changes the gain of the $S$ branch so that $C_a$ the opponent signal from the adapting color is kept close to zero, i.e. close to the least compressed part of the response curve. Difference thresholds are smallest when $C_{a+f}$ is close to zero; a larger difference between the probe and the flash is needed to achieve a unit response difference when $C_{a+f}$ is considerably larger or smaller than zero.

The sets of difference thresholds for different states of adaptation have widely varying distributions. For example, a much larger difference is needed at threshold on a "violet" judgment point when adapted to a "yellow" than on a "yellow" judgment point when adapted to a "violet." Consistent with data, the model predicts shallower curves to the negative side of all adapting lights than to the positive side. This prediction is a consequence of assuming a static response function whose shape is not altered by adaptation conditions.

Data from the second observer in Fig. 12 show the same effects. There was a clear tendency for difference thresholds to be smallest when the observer was adapted to the color where the judgment was made. The curves are predictions from the model using the same parameters as the first observer. A comparison of the points to the curves provides an estimate of inter-observer variability.

## EXPERIMENT 4

Experiment 4 was designed to test the opponent assumptions of the model by measuring $S$ probe decrement thresholds for $LM$ flashes from the same adapting backgrounds as in Expt 3. As shown in Fig. 9, the conditions of Expt 3 stimulated only the $S$ branch of the pre-opponent $S$-cone system. The skeletal diagram in Fig. 13 shows that in Expt 4, the change in steady adaptation ($\Delta$a) changed the state of the $S$ branch, but not the $LM$ branch. The change from each steady background to the flash ($\Delta$f) was registered by the $LM$ branch but not the $S$ branch. The probes were pure $S$ decrements from the flash, so $\Delta$p was detected exclusively through the $S$ branch. The adapting backgrounds are shown as letters "a–h" on the color diagram in Fig. 14. The asterisks on the vertical lines through the adapting color represent the positions of the flashes for each steady background. The flashes were thus pure $LM$ increments or decrements from the adapting background. The flashes used for different adaptation colors were limited by the range of the equipment and the sensitivity of the visual system.

The measurements of difference thresholds for observer AS are shown in Fig. 15. The panels (a)–(h) show the data for the corresponding adaptation points in Fig. 14. Flashes are plotted along the horizontal axis in negative $\Delta(L+M)$ excursions from the adapting point, and thresholds along the vertical axis as negative $\Delta S$ changes from the flashes. The empirical threshold curves

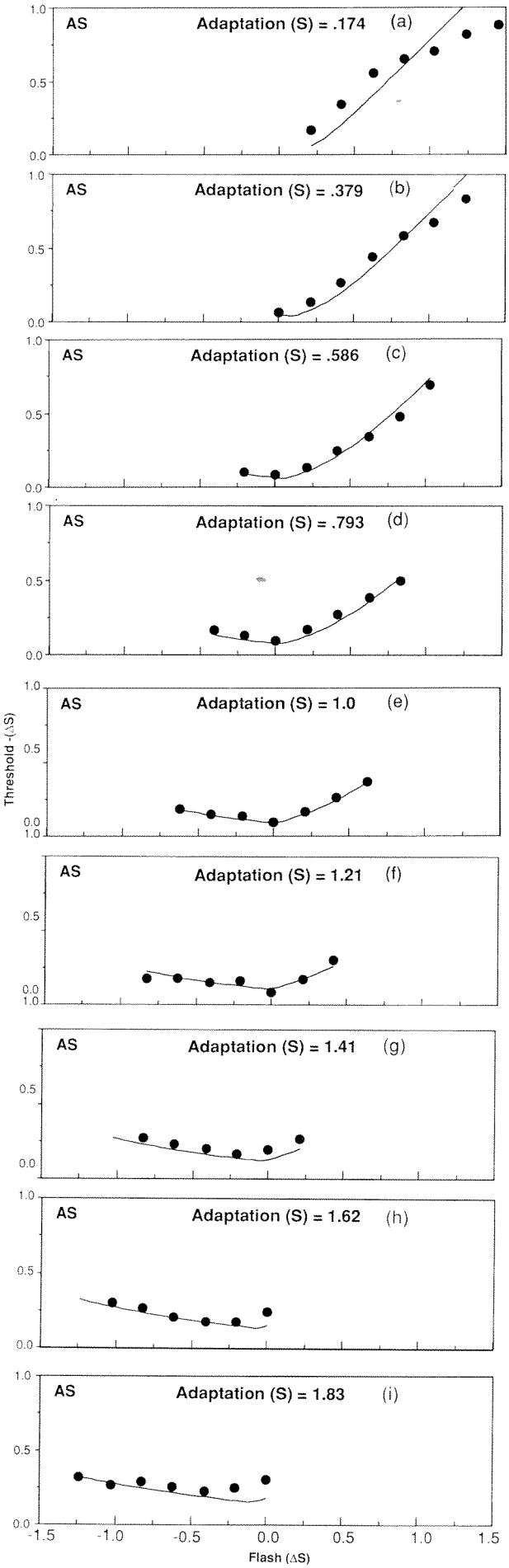


FIGURE 11. Results for observer AS from Expt 3. (a)–(i) show the difference thresholds as a function of the judgment point's increment or decrement from the adapting field in $\Delta S$ units. The scale of the flash for all panels is shown at the bottom of (i). Each panel represents adaptation to a different steady field along the "yellow–violet" line. The location of the adapting field in the color plane is shown in Fig. 10 by each panel's label. The solid lines represent the predictions of the model with all parameters previously determined.

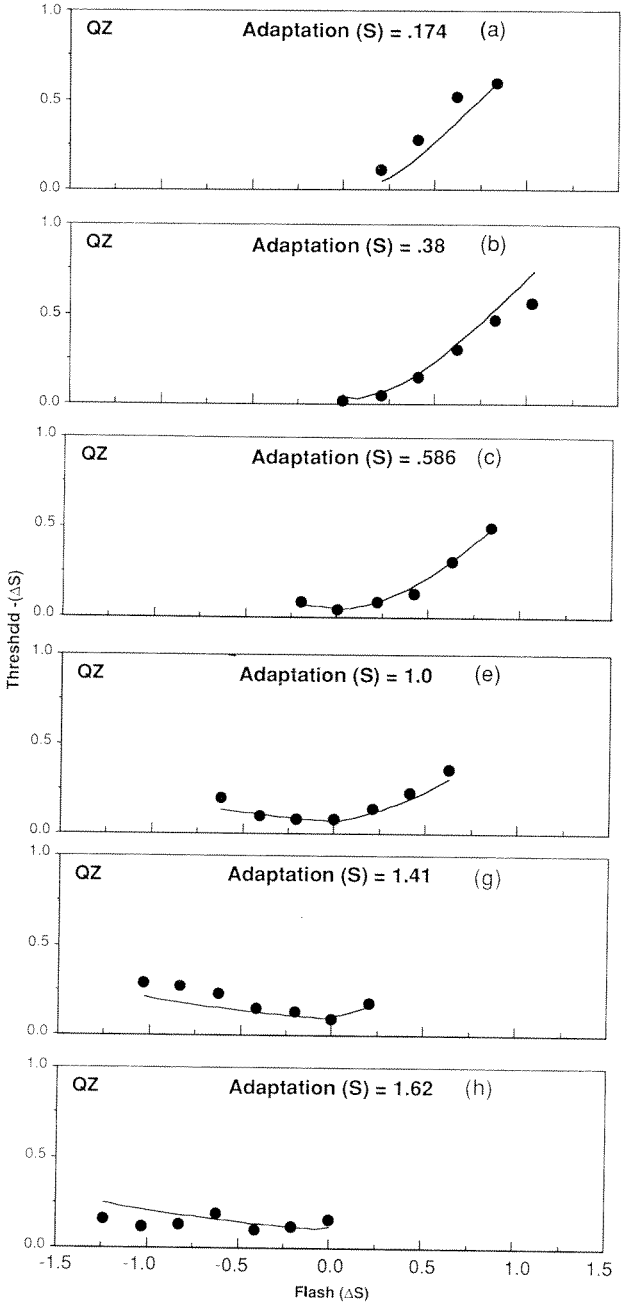


FIGURE 12. Results from Expt 3 for observer QZ, plotted similarly to Fig. 11. The solid lines represent the predictions of the model with the parameters estimated for AS.

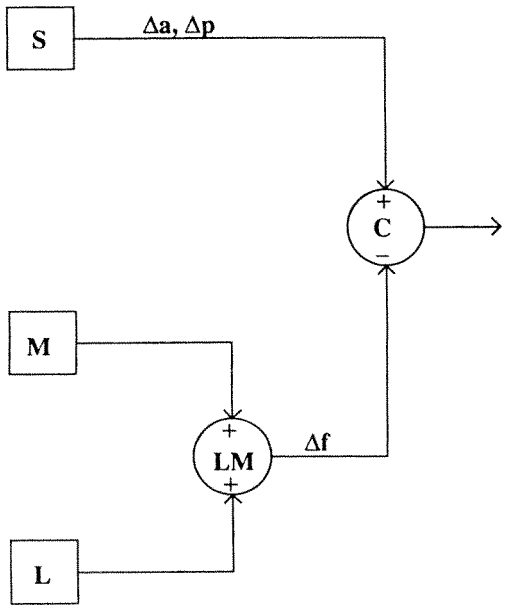


FIGURE 13. The effect of the lights in Expt 4 shown on the skeletal model of the $S$-cone system. "Δa" identifies those branches of the system affected by a change between the steady adapting fields. "Δf" identifies those branches of the system affected by a change from the steady field to the flashed field. "Δp" identifies those branches of the system affected by a change from the flashed field to the probe.

in Fig. 15 have different shapes than the curves for the same adaptation conditions in Fig. 11. However, the minimum thresholds are at or near the adaptation point in all the panels in both figures. The solid curves represent the predictions from the model for the conditions of this experiment. There seems to a reasonable concordance between the data and the model supporting the model's assumption that the static compressive nonlinearity is located following the opponent combination of $S$ and $LM$ signals. If static nonlinearities were located independently in the $S$ and $LM$ branches, the model would seriously underestimate the difference thresholds measured against $LM$ flashes.

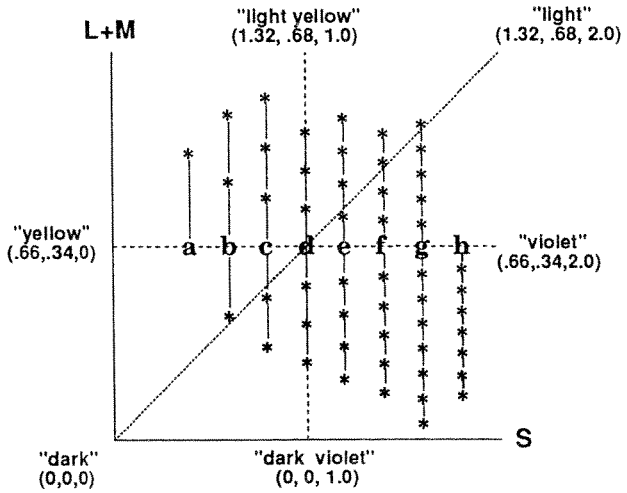


FIGURE 14. Adapting and flash conditions for Expt 4. The letters "a–h" depict the locations of the steady adapting field. The asterisks, depict the location of the flashed fields used as judgment points for each adaptation condition. The flashed fields were $L + M$ increments or decrements from the adapting background.

Data from the second observer are plotted in Fig. 16. The curves are predictions from the model using the parameter values estimated for the first observer. The data for the two observers are reasonably similar, and the model reproduces the main features in the data from the second observer.

## EXPERIMENT 5

An important assumption of the model is the equal weight given to the $S$ and $L + M$ signals at the opponent combination. Coupled with the scales of the $S$ and $L + M$ axes in Fig. 2, this assumption implies a zero opponent signal for all lights along the diagonal "light–dark" line through W. The model therefore predicts that at steady adaptation to W the $S$-cone system will give zero transient responses to flashes on the "light–dark" line. Difference thresholds for discriminating $S$ probes from these judgment colors should all be equal. In fact the model predicts approximately flat curves for "radiance" flashes through any adapting color on the horizontal axis (i.e. flashes on the line joining the adapting color and the "dark" point). These issues relate to the combination of transient signals from the two pre-opponent branches and were tested in Expt 5. The skeletal diagram in Fig. 17 shows that in this experiment flashed changes affected both pre-opponent branches and changes in steady adaptation affected only the $S$ branch. The adapting and flashed stimuli are shown in Fig. 18. The letters "a–h" represent the adapting backgrounds. The asterisks on the lines through each adapting point represent the flashed changes from each background. The flashes were equal in $\Delta S$ changes to the flashes in Expt 3 and in $\Delta(L + M)$ changes to the flashes in Expt 4. The probes were $S$-cone decrements from the flashed fields.

The results for observer AS are plotted in Fig. 19. The thresholds are in negative $\Delta S$ units. The flashed changes are in units of retinal illuminance expressed as fractions of 49.5 cd/m$^2$ (the luminance of the adapting lights). The solid curves are predictions from the model. The threshold data are flatter than in Expts 3 and 4, and the flat predicted curves generally resemble the data. However, in Fig. 19(c, d, e) whereas the predicted curves are flat, the data have a shallow but distinct V shape. The most pronounced deviations are for the positive flashes in Fig. 19(d), i.e. adaptation to W. The data for the second observer, plotted in Fig. 20, showed the same pattern.

A number of simple factors can be ruled out as a source of the discrepancy between the data and the model's predictions. Because the threshold elevations in Fig. 19(d) are larger than those for corresponding changes of steady "light–dark" adaptation in Fig. 5(c), it is unlikely that the threshold elevations are due to the adaptation state being altered by the flashes. The V shaped nature of the data also rules out the possibility that the threshold elevations are due to a pre-opponent static compressive nonlinearity. The magnitude of the elevations makes it unlikely that a minor calibration

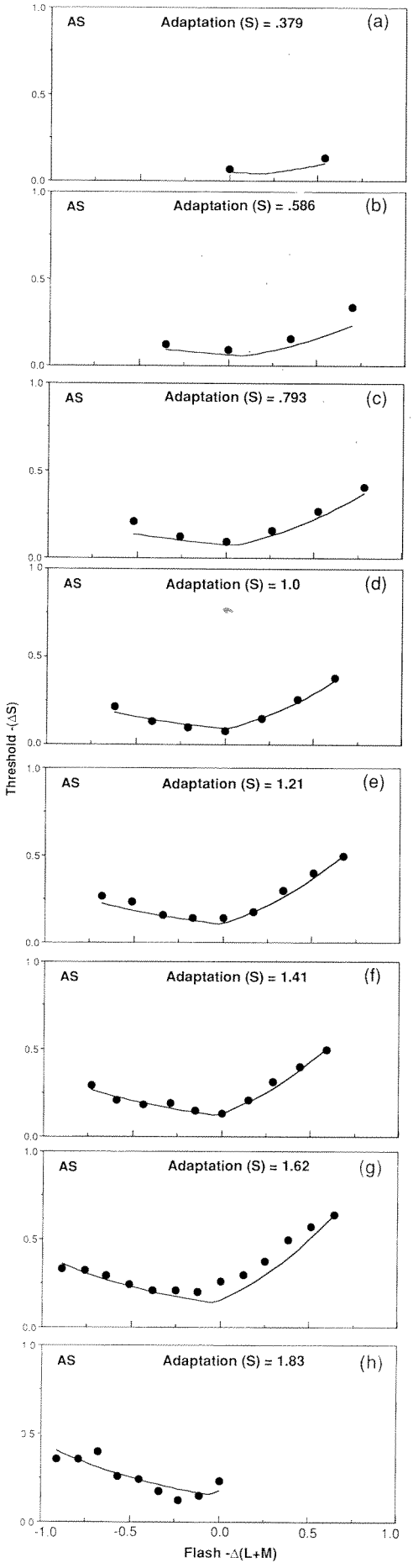


FIGURE 15. *Caption on facing page.*

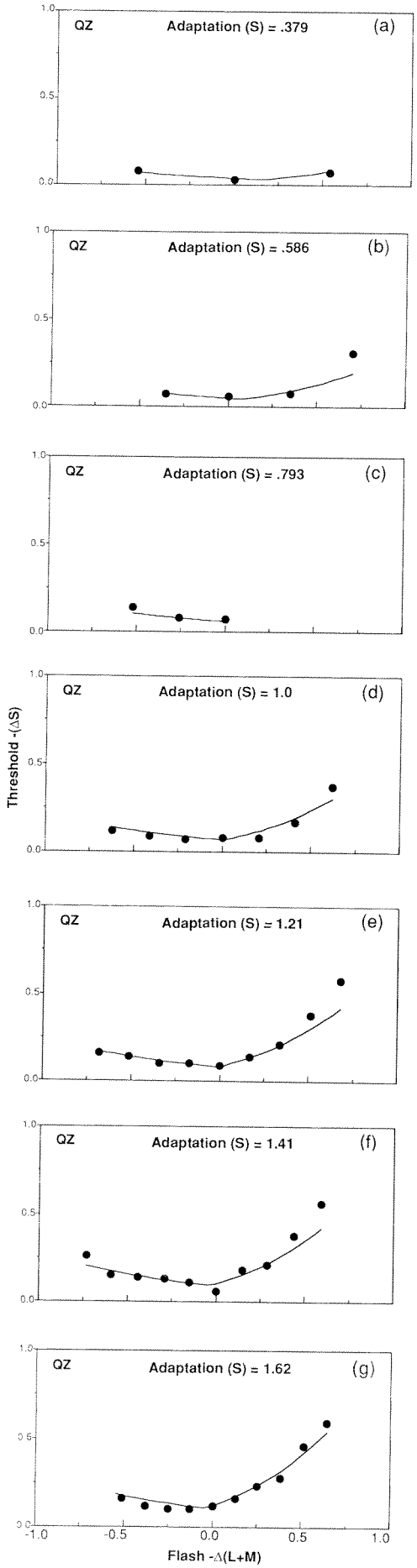


FIGURE 16. *Caption on facing page.*

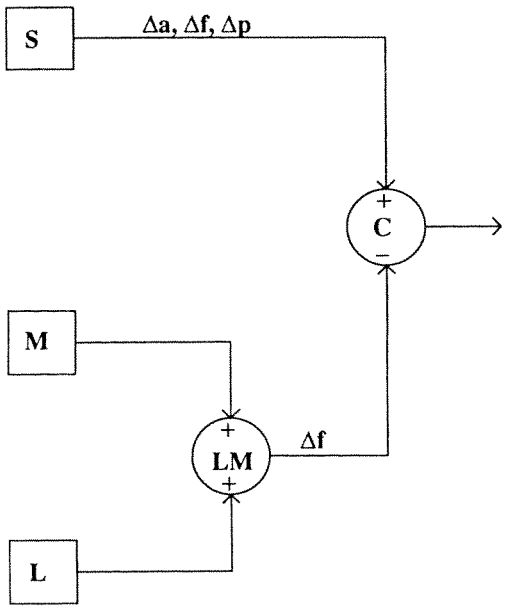


FIGURE 17. The effect of the lights in Expt 5 shown on the skeletal model of the $S$-cone system. "Δa" identifies those branches of the system affected by a change between the steady adapting fields. "Δf" identifies those branches of the system affected by a change from the steady field to the flashed field. "Δp" identifies those branches of the system affected by a change from the flashed field to the probe.

error about the chromaticity of lights on the "light–dark" line is responsible. The most probable cause is that the two pre-opponent branches have different spatial and temporal properties, and transient "radiance" flashes evoke transiently non-zero opponent signals due to these differences.

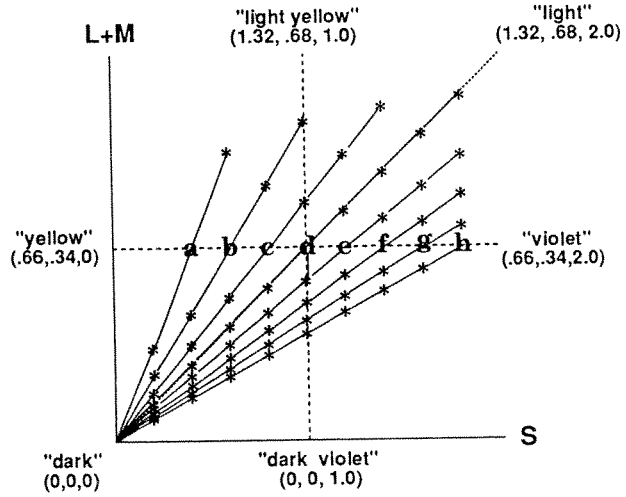


FIGURE 18. Adapting and flash conditions for Expt 5. The letters "a–h" depict the locations of each of the adapting fields. The asterisks depict the location of the flashed fields used as judgment points for each adaptation condition. The flashes were increments or decrements from the adapting field in the direction of "dark".

## EXPERIMENT 6

Experiment 6 was designed to test the assumption that $\kappa$, the multiplicative gain constant, is identical for the $S$ and $LM$ pre-opponent branches. This assumption was tested by shifting the observer's adaptation along the "light–dark" diagonal, thus changing the multiplicative gain factor in both pre-opponent branches. For steady-state thresholds, this assumption is consistent with the results shown in Fig. 5(c). For difference thresholds at flashed judgment points, the conditions in this experiment are schematized in the skeletal diagram in Fig. 21. The colors of the adapting and flashed lights are shown in the color diagram in Fig. 22. The flashes were pure $S$ changes from the adapting field, i.e. parallel to the horizontal axis. The probes were $S$ decrements from the flashes.

The results of changing "light–dark" adaptation for observer AS are shown in Fig. 23. The flashed changes are plotted in $\Delta S$ units and the thresholds in negative $\Delta S$ units. The minimum threshold in each panel is again at the steady adaptation level. The model's predictions and the data agree reasonably well. If the multiplicative constants in the two pre-opponent branches were appreciably different, the minimum difference threshold should shift away from the "light–dark" line. Therefore under these experimental conditions the two pre-opponent branches seem to change state in a similar fashion in response to a change in steady state adaptation. Since it is possible that the spatial and temporal properties of the two branches are different, the relative states of the two adaptive mechanisms may depend not only on the spectral but also on the spatio-temporal characteristics of the stimuli. In the present experiments, where the observer adapted for a prolonged period to a large 10° square field, a single value of $\kappa$ seems reasonable and simplifies the model.

## SUMMARY AND DISCUSSION

The experiments in this study were an attempt at a psychophysical dissection of the $S$-cone color system. The results are consistent with the following components at the initial stages of the $S$-cone system. The first stage consists of the $S$, $M$, and $L$-cones which function as linear transducers of light. The outputs of the $L$- and $M$-cones are added to give an $LM$ signal. The $S$ and $LM$ signals independently pass through similar multiplicative

FIGURE 15 (*opposite*). Results for observer AS from Expt 4. (a)–(h) show the difference thresholds as a function of the judgment point's increment or decrement from the adapting field in $-\Delta(L+M)$ units. The scale of the flash for all panels is shown at the bottom of (h). Each panel represents adaptation to a different steady field along the "yellow–violet" line. The location of the adapting field in the color plane is shown in Fig. 13 by each panel's label. The solid lines represent the predictions of the model.

FIGURE 16 (*opposite*). Results from Expt 4 for observer QZ, plotted similarly to Fig. 15. The solid lines represent the predictions of the model with the parameters estimated for AS.

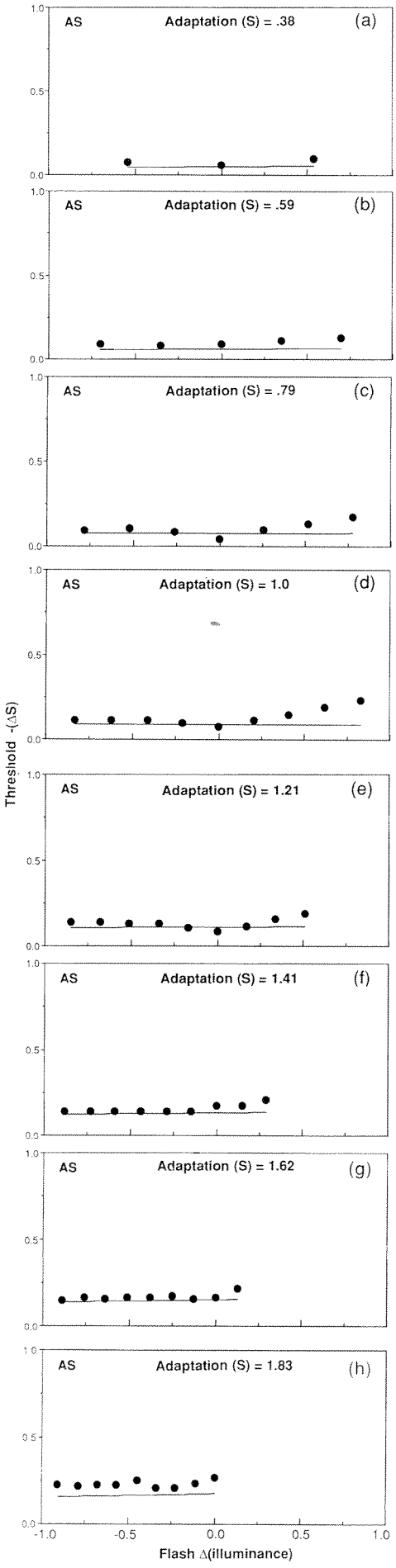


FIGURE 19. *Caption on facing page.*

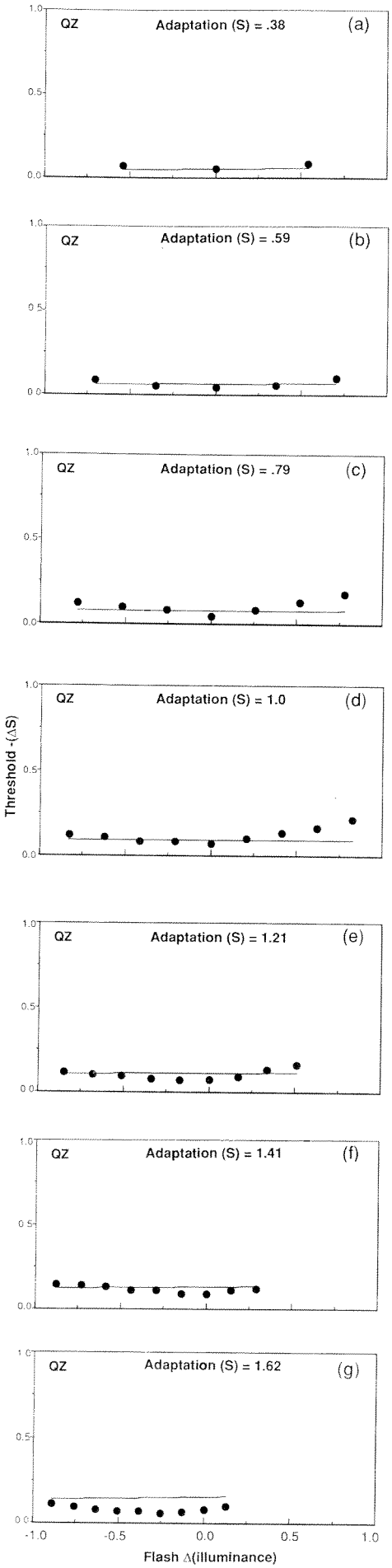


FIGURE 20. *Caption on facing page.*

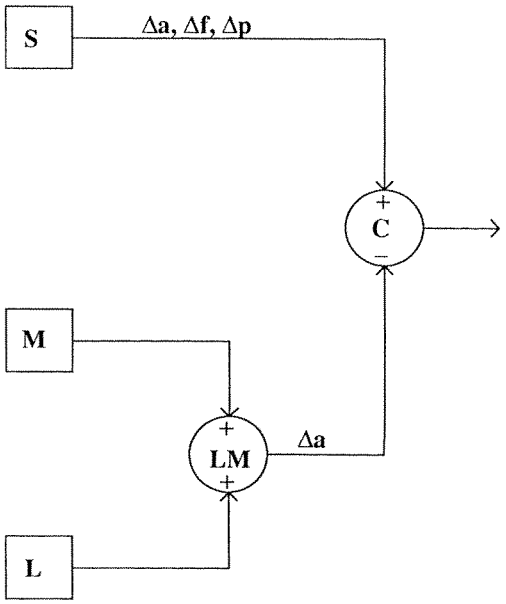


FIGURE 21. The effect of the lights in Expt 6 shown on the skeletal model of the *S*-cone system. "Δa" identifies those branches of the system affected by a change between the steady adapting fields. "Δf" identifies those branches of the system affected by a change from the steady field to the flashed field. "Δp" identifies those branches of the system affected by a change from the flashed field to the probe.

adaptive mechanisms. The gain of each mechanism is a monotonically decreasing function of the steady adapting signal in that branch. The gain-adjusted *S* signal minus the gain-adjusted *LM* signal constitutes an opponent chromatic signal *C*. Equal weights at the opponent combination together with similar gain controls

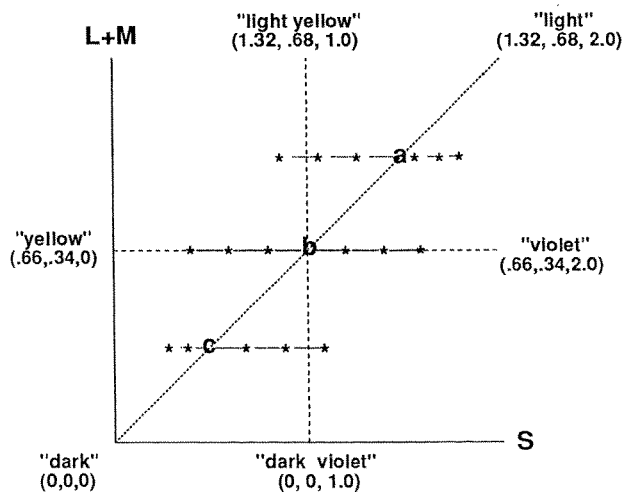


FIGURE 22. Adapting and flash conditions for Expt 6. The letters a, b and c along the "light–dark" line depict the location of the adapting fields. The asterisks connected by dashed lines to each letter depict the location of the flashed fields. The flashed fields are pure *S* changes from the adapting background.

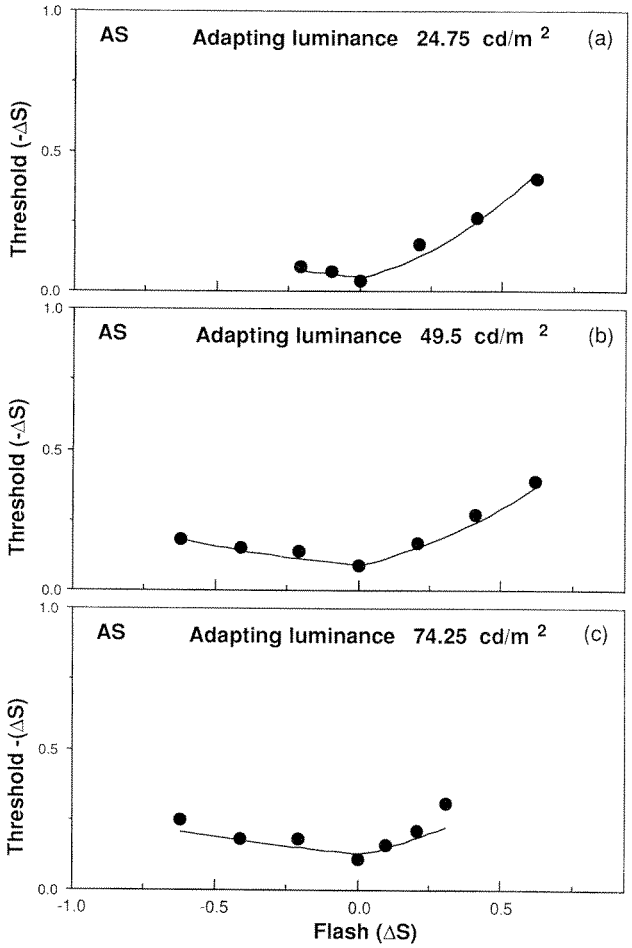


FIGURE 23. Results for observer AS from Expt 6. In (a)–(c) the difference thresholds are plotted vs increments or decrements of the flash from the adapting field in changes in Δ*S* units. The scale of the flash for all panels is shown at the bottom of (c). Each panel represents adaptation to a different steady field along the "light–dark" line. The location of the adapting field in the color plane is shown in Fig. 18 by each panel's label. The solid lines represent the predictions of the model.

lead to a zero opponent signal for all steady lights metameric to equal energy white. The opponent signal passes through a static mechanism whose output is a sign and null preserving sigmoidal function of the opponent signal. The response function is more compressed on the positive than the negative side. In this model, the *L* and *M* signals are combined into an *LM* signal purely for conceptual convenience. A model with independent gain controls in the *L* and *M* branches and only one site of signal combination at *C* would be equally compatible with the results of this study.

When changes in adaptation state were restricted to changes in the *S*-cone system by adapting the observer to lights of constant *L*- and *M*-cone excitation, thresholds increased as a function of the *S*-cone

FIGURE 19 (*opposite*). Results for observer AS from Expt 5. In (a)–(h) the difference thresholds are plotted vs increments or decrements of the flash from the adapting field in changes in retinal illuminance expressed as fractions of 49.5 cd/m$^2$. The scale of the flash for all panels is shown at the bottom of (h). Each panel represents adaptation to a different steady field along the "yellow–violet" line. The location of the adapting field in the color plane is shown in Fig. 18 by each panel's label. The solid lines represent the predictions of the model.

FIGURE 20 (*opposite*). Results from Expt 5 for observer QZ, plotted similarly to Fig. 19. The solid lines represent the predictions of the model with the parameters estimated for AS.

excitation from the steady backgrounds. The function was not linear [Fig. 5(a)]. The model correctly predicted lines of different slope on the two sides of W, but underestimated the thresholds on the "violet" side. When the observer was adapted to achromatic colors of different luminance, the function relating the threshold $S$-cone difference between the probe and the background and the $S$-cone excitation from the background was linear, as predicted by the model [Fig. 5(c)]. A comparison of Fig. 5(a) to Fig. 5(c) shows that $S$-cone thresholds were lower on achromatic backgrounds than on "yellow" or "violet" lights of equivalent $S$-cone excitation whose chromaticities fall on the horizontal axis through W. These results can be explained by the model as follows: All steady lights in Fig. 5(c) along the achromatic "light–dark" line have equal $S$ and $L + M$ components and thus give a zero opponent response in the model. Consequently, an $S$-probe has to be a sufficient decrement to reduce the response fom 0 to $-1$ in the static nonlinear process. For steady lights along a horizontal line as in Fig. 5(a), however, $S$ is not equal to $L + M$ (except at W), so that there is a non-zero opponent signal from the background and the $S$ decrement has to be sufficient to reduce the response of the static nonlinear process by 1 from a point other than 0. Because of the compressive shape of the nonlinear curve on both sides of white, thresholds are higher on "violet" or "yellow" backgrounds than on chromatically neutral backgrounds of equivalent $S$-cone excitation. In Fig. 5(b), adaptation was shifted so that only the $L + M$ signal from the adapting light changed while the $S$ signal was constant. Under these conditions, thresholds were fairly constant. Because a change in steady adaptation along the $L + M$ line changes the gain of the $LM$ branch but not of the $S$ branch, the $S$ probe signals in all these conditions are multiplied by the same gain. Consequently, threshold changes in this condition could only be due to a non-zero opponent signal from the steady background. The model's predictions agree with the data for most of the backgrounds in Fig. 5(b), but overestimate the opponent signal from the "darkest-violet" field. In an informal sensitivity analysis of the model, it was found that the multiplicative parameter $\kappa$ could be changed within a small range without appreciably changing the fit to the "light–dark" data in Fig. 5(c). Increasing $\kappa$ improved the fit to the data in Fig. 5(a) but made the fit to the data in Fig. 5(b) worse. Decreasing $\kappa$ had the opposite effect. Within the parameters of this simple model it was not possible to simultaneously improve the fit in both Fig. 5(a) and (b).

In most states of adaptation, the lowest thresholds are generally for the zero flash condition (Figs 11, 12, 15, 16, 19, 20, 23). In other words, the sensitivity of the $S$-cone system shifts so that the best discrimination is in the neighbourhood of the adaptation color. The model explains this behavior by a combination of the pre-opponent multiplicative gain controls and the nonlinear shape of the post-opponent response curve. The adaptive processes independently multiply the signals in the $S$ and $LM$ branches by scalars that are decreasing functions of the steady signals within each branch. The effect is to reduce the absolute value of the difference between the steady $S$ and $LM$ signals, i.e. to shift the opponent input to the static mechanism towards zero. Since the smallest input difference required for a unit response difference is around zero opponent input, difference thresholds will be lowest at the adapting light or at a short distance towards W from the adapting light, depending on the parameter $\kappa$.

Since this model provides a good description of the $S$-cone system for the range of stimuli studied in this paper, it is worth relating it to phenomena associated with the $S$-cone system. Other attempts to study sensitivity control in the $S$-cone system with flashed backgrounds, have come to conclusions that are only in partial agreement with the present model. In agreement, previous work presented evidence consistent with a static nonlinearity after the opponent combination; e.g. adding a "yellow" flash to a "blue" flash decreased the difference threshold for a blue probe (Stromeyer, Kronauer & Madsen, 1978, 1979; Benimoff & Hood, 1983). Further, adaptive changes attributed to a multiplicative process, were needed at the pre-opponent stage (Benimoff & Hood, 1983). Unlike the present results, these same studies also found evidence compatible with static nonlinearities in the pre-opponent branches. It is possible that the larger range of flashes used in the earlier studies are conditions that reveal first stage nonlinearities.

The phenomenon termed "transient tritanopia" by Mollon and Polden (1977) refers to the transient elevation in the absolute threshold for detecting short-wavelength probes after a long-wavelength adapting background is turned off. In this study, the condition that could reveal this phenomenon would be adaptation to "yellow" and a flash that was a radiance decrement equal to the radiance of the adapting light. However, there are no probes that could be equiluminant tritanopic confusion pairs with "dark". Therefore, the closest conditions are shown in Figs 19(a) and 20(a). Under these conditions $S$-cone difference thresholds were not elevated by the flash. It is likely that adapting lights of greater radiance or a larger flashed decrement are required to obtain transient tritanopia. In its present form, the model is not sufficient to predict transient tritanopia. In fact without assuming a substantial amount of "dark-noise", no form of multiplicative gain controls is sufficient to explain some classes of post-adaptation phenomena that occur on dark backgrounds, i.e. in the absence of input to the visual system. These phenomena include transient tritanopia and the appearance of complementary after-images in the dark. Such phenomena are consistent with adaptive mechanisms that accumulate a steady neutralizing signal to adapting lights, e.g. the subtractive mechanism proposed by Jameson and Hurvich (1972). Given a linear opponent combination of cone signals, it is not possible to localize these mechanisms as pre- or post-opponent by psychophysical means.

The model can, however, explain the transient elevation of thresholds along the constant $L\&M$ line shown by Krauskopf, Williams, Mandler and Brown (1986). Krauskopf *et al.* (1986) compared pure $S$-cone

increment and decrement thresholds on a steady mid-white background to thresholds on the same background after a 1.0 sec exposure to adapting lights on the ends of the "yellow–violet" axis of Fig. 2. In terms of the present conceptual scheme, the 1.0 sec exposure shifts the observer's adaptation toward "yellow" or "violet". The threshold elevation is similar to the increase in $\Delta S$ thresholds for judgments at W when the observer's adaptation shifts to either "yellow" or "violet" compared to when the observer is adapted to W. If the thresholds in each panel of Fig. 11 were plotted vs the chromaticity of the judgment points (adapting, background + flash), the curves belonging to different panels would mainly be laterally shifted versions of each other. In Fig. 11 panels (a)–(d) the thresholds at W will be to the left of the minimum point whereas in panels (f)–(i) they will be to the right. The change in the threshold at W corresponds to the mainly lateral shift of the threshold curves, and is adequately explained by the model.

Another phenomenon that may be partially explainable by the model is Tyndall's (1933) result that wavelength discrimination around 455 nm improved when the saturation of the test fields was reduced. In the present model, the response of the sensitivity limiting mechanism is a function of the opponent signal, therefore combination with lights that decrease saturation will reduce the difference between the $S_a$ and $LM_a$ signals and lead to smaller $\Delta S$ thresholds. To the extent that the $S$-cone system contributes to wavelength discrimination around 455 nm, the magnitude of $\Delta\lambda$ will decrease with decreasing saturation.

The two types of mechanisms incorporated in the model cannot explain why exposure to prolonged temporal modulation of colors along the $S$-cone axis raises thresholds for pure $S$ probes (Krauskopf *et al.*, 1982). On the basis of preliminary data, this effect seems to require a post-opponent multiplicative mechanism whose gain is a function of the properties of the habituating modulation (Shapiro & Zaidi, 1991).

The model is concerned with the sensitivity of only the $S$-cone system; therefore, it is not designed to explain phenomena based on the subjective impression of colors like "unique" hues or the Abney and Bezold–Brucke effects. However, the model does predict one aspect of subjective appearance that involves only the $S$-cone system. If a sine-wave along the "yellow–violet" axis is the input to the model, the output will be a flattened wave due to the sigmoidal response function. This is consistent with the perceived appearance of both temporal and spatial equi-luminant "yellow–violet" sine-waves.

The model proposed in this paper is extremely simple due to the use of a number of strict assumptions. However, the requirements that the shape of the response function be invariant and that the weights of signal combination not depend on adaptation state may be too rigid. In addition, all adaptation is approximated by simple pre-opponent multiplicative processes. A number of other types of processes could have been added to the model, e.g. pre-opponent static non-linearities or post-opponent subtractive or multiplicative adaptive processes. The results of the present experiments did not indicate the need for these additional processes, and adding them to the model did not improve the overall fit to the data. This model's ability to explain the $S$-cone system's sensitivity for lights of different colors than the adapting lights, makes it more general than the "static" model of Pugh and Mollon (1979) that was designed to account for discrimination thresholds at adapting points only. In the present model, with a static non-linearity, the increment required for threshold is a function of the magnitude of the instantaneous response of the opponent stage; wherease in Pugh and Mollon's model, the increment is controlled by the net steady-state signal of the opponent stage. Because of the spatial and temporal configurations of the stimuli used in this study, it was possible to make the gain solely a function of the steady background, and the response solely a function of the instantaneous input. For more general conditions, temporal and spatial factors would have to be incorporated in the model, like in the dynamic model of Pugh and Mollon (1979). Given that the model is parsimonious, that the particular mathematical functions were chosen for analytical convenience, and that the values of the parameters were fixed after being estimated from just two out of a large set of experimental conditions, the processes embodied in the model seem to provide a good explanation for the differential sensitivity of the $S$-cone system for a wide range of steady adapting stimuli.

## REFERENCES


Adelson, E. A. (1982). Saturation and adaptation in the rod system. *Vision Research, 22*, 1299–1312.

Benimoff, N. I. & Hood, D. C. (1983). A comparison of adaptation of the R/G and B/Y pathways. *Investigative Opthalmology and Visual Science (Suppl.), 24*, 205.

Boynton, R. M. (1979). *Human color vision*. New York: Holt (Rinehart & Winston).

Brindley, G. S. (1970). *Physiology of the retina and visual pathway* (2nd edn). Baltimore: Williams & Wilkins.

Brown, W. R. J. (1952). The effect of field size and chromatic surroundings on color discrimination. *Journal of the Optical Society of America, 42*, 837–844.

Burns, S. A., Elsner, A. E., Pokorny, J. & Smith, V. C. (1984). The Abney effect: Chromaticity coordinates of unique and other constant hues. *Vision Research, 24*, 479–489.

*CIE Proceedings* (1931). Cambridge: Cambridge University Press.

Craik, K. J. W. (1938). The effect of adaptation on differential brightness discrimination. *Journal of Physiology, London, 92*, 406–421.

Crawford, B. H. (1946). Visual adaptation in relation to brief conditioning stimuli. *Proceedings of the Royal Society of London, Series B, 134*, 283–302.

Dawis, S. M. (1981). The compression model: A re-examination. *Vision Research, 21*, 1511–1515.

Dimmick, F. L. & Hubbard, M. R. (1939a). The spectral location of psychologically unique yellow, green and blue. *American Journal of Psychology, 52*, 242–254.

Dimmick, F. L. & Hubbard, M. R. (1939b). The spectral components of psychologically unique red. *American Journal of Psychology, 52*, 348–353.

Donders, F. C. (1881). Uber Farbensysteme. *Albrecht V. Graefes. Archiv für Ophthalmologie, 27*, 155–223.

Finkelstein, M. A. & Hood, D. C. (1981). Cone system saturation: More than one stage of sensitivity loss. *Vision Research, 21*, 319–328.

Finkelstein, M. A., Harrison, M. & Hood, D. C. (1990). Sites of sensitivity control within a long-wavelength cone pathway. *Vision Research, 30*, 1145–1158.

Geisler, W. S. (1978). Adaptation, afterimages and cone saturation. *Vision Research, 18*, 279–289.

Geisler, W. S. (1979). Initial image and after image discrimination in the human rod and cone system. *Journal of Physiology, London, 294*, 165–179.

Geisler, W. S. (1981). Effects of bleaching and backgrounds on the flash response of the cone system. *Journal of Physiology, London, 312*, 413–434.

Geisler, W. S. (1983). Mechanisms of visual sensitivity: Backgrounds and early dark adaptation. *Vision Research, 23*, 1423–1432.

Guth, S. L. & Lodge, S. L. (1973). Heterochromatic additivity, foveal spectral sensitivity and a new color model. *Journal of the Optical Society of America, 63*, 450–462.

Hayhoe, A. A., Benimoff, N. I. & Hood, D. C. (1987). The time-course of multiplicative and subtractive adaptation process. *Vision Research, 27*, 1981–1996.

Heinemann, E. G. (1961). The relation of apparent brightness to the threshold for differences in luminance. *Journal of Experimental Psychology, 61*, 389–399.

Hering, E. (1878). *Zur Lehre vom Lichtsinne*. Wien: Carl Gerold's Sohn.

Hood, D. C. (1978). Psychophysical and physiological tests of proposed mechanisms of light adaptation. In Armington, J., Krauskopf, J. & Wooten, B. (Eds), *Visual psychophysics: Its physiological basis*. New York: Academic Press.

Hood, D. C. & Greenstein, V. C. (1982). An approach to testing alternative hypotheses of changes in visual sensitivity due to retinal disease. *Investigative Ophthalmology and Visual Science, 23*, 96–101.

Hood, D. C., Finkelstein, M. A. & Buckingham, E. (1979). Psychophysical tests of models of the response function. *Vision Research, 19*, 401–406.

Hood, D. C., Ilves, T., Maurer, E., Wandell, B. & Buckingham, E. (1978). Human cone saturation as a function of ambient intensity: A test of models of shifts in the dynamic range. *Vision Research, 18*, 983–993.

Hurvich, L. M. & Jameson, D. (1961). Opponent chromatic induction and wavelength discrimination. In Jung, R. & Kornhuber, H. (Eds), *The visual system: Neurophysiology and psychophysics* (pp. 144–152).

Jameson, D. & Hurvich, L. M. (1972). Color adaptation: Sensitivity, contrast and afterimages. In Jameson, D. & Hurvich, L. M. (Eds), *Handbook of sensory physiology: Visual psychophysics* (VII/4, pp. 568–581). Berlin: Springer.

Ingling, C. R. (1977). The spectral sensitivity of the opponent-color channels. *Vision Research, 17*, 1083–1089.

King-Smith, P. E. & Webb, J. R. (1970). The use of photopic saturation in determining the fundamental spectral sensitivity curves. *Vision Research, 14*, 421–429.

Konig, A. & Dieterici, C. (1893). Die Grundempfindungen in normalen and anomalen Farben Systemen und ihre Intensitats—Verteilung in Spectrum. *Zeitschrift für Psychologie und Physiologie der Simesorgane, 4*, 241–347.

Krauskopf, J., Williams, D. R. & Heely, D. M. (1982). The cardinal directions of color space. *Vision Research, 2*, 1123–1131.

Krauskopf, J., Williams, D. R., Mandler, M. B. & Brown, A. M. (1986). Higher order color mechanisms. *Vision Research, 26*, 23–32.

von Kries, J. (1905). Die Gesichtsempfindungen. Nagel, W. (Ed), *Handbook der Physiologie des Menschen, 3*, 102–282.

Larimer, J., Krantz, D. H. & Cicerone, C. M. (1975). Opponent-process additivity. I. Yellow/Blue equilibria and non-linear models. *Vision Research, 18*, 723–731.

Loomis, J. M. & Berger, T. (1979). Effects of chromatic adaptation on color discrimination and color appearance. *Vision Research, 19*, 891–901.

Lythgoe, R. J. (1936). *Transactions of the Illuminating Engineering Society, 1*, 3.

MacLeod, D. I. A. & Boynton, R. M. (1978). Chromaticity diagram showing cone excitation by stimuli of equal luminance. *Journal of the Optical Society of America, 69*, 1183–1186.

Maxwell, J. C. (1860). On the theory of compound colours and the relations of the colours of the spectrum. *Philosophical Transactions of the Royal Society, 150*, 57–84.

Mollon, J. D. (1982). Color vision. *Annual Review of Psychology, 33*, 41–85.

Mollon, J. D. & Polden, P. G. (1977). An anomaly in the response of the eye to light of short wavelengths. *Philosphical Transactions of the Royal Society of London, Series B, 278*, 207–240.

Pointer, M. R. (1974). Color discrimination as a function of observer adaptation. *Journal of the Optical Society of America, 64*, 750–759.

Pokorny, J., Smith, V. C., Burns, S. A., Elsner, A. & Zaidi, Q. (1981). Modeling blue-yellow opponency. In Richter, M. (Ed.), *Proceedings 4th congress of the international color association*. Berlin: AIC.

Pugh, E. N. (1976). The nature of the pi1 mechanism of W. S. Stiles. *Journal of Physiology, London, 83*, 713–747.

Pugh, E. N. & Mollon, J. D. (1979). A theory of the pi 1 and pi 3 color mechanisms of Stiles. *Vision Research, 19*, 293–312.

Schrodinger, E. (1925). Uber das Verhaltnis der Vierfarben zur Dreifarbentheorie. *Sitzungsbergichte der Akademie der Wissenschaften in Wien (Mathematisch-Naturwissenschaftliche Klasse Abteilung 2a), 134*, 471.

Shapiro, A. G. & Zaidi, Q. (1991). The effects of prolonged temporal modulation on the response of color mechanisms. *Investigative Ophthalmology and Visual Science (Suppl.), 32*, 94.

Shevell, S. K. (1977). Saturation in human cones. *Vision Research, 17*, 427–434.

Smith, V. C. & Pokorny, J. (1975). Spectral sensitivity of the foveal cone pigments between 400 and 500 nm. *Vision Research, 15*, 161–171.

Stiles, W. S. (1939). The directional sensitivity of the retina and the spectral sensitivities of the rods and cones. *Proceedings of the Royal Society of London, Series B, 127*, 64.

Stiles, W. S. (1949). Increment thresholds and the mechanisms of colour vision. *Documenta Ophthalmologica, 3*, 138–163.

Stiles, W. S. (1953). Further studies of visual mechanisms by the two-colour threshold technique. *Coloquis Sobre Problemas Opticos de la Vision: Conferancias Generales. I. Union Internationale de Physique Pure et Appliquée, 1*, 65–103 (U.I.P.A.P., Madrid).

Stiles, W. S. (1959). Color vision: The approach through increment threshold sensitivity. *Proceedings of the National Academy of Science, U.S.A. 45*, 100–114.

Stiles, W. S. (1967). Mechanism concepts in colour theory. Newton Lecture. *Journal of Colour Group, 11*, 106–123.

Stiles, W. S. (1978). *Mechanisms of colour vision*. London: Academic Press.

Stockman, A., MacLeod, D. I. A. & DePriest, D. D. (1991). The temporal properties of the human shortwave photoreceptors and their associated pathways. *Vision Research, 31*, 189–208.

Stromeyer III, C. F., Kronauer, R. E. & Madsen, J. C. (1978). Apparent saturation of blue-sensitive cones occurs at a color-opponent stage. *Science, 202*, 217–219.

Stromeyer III, C. F., Kronauer, R. E. & Madsen, J. C. (1979). Response saturation of short-wavelength cone pathways controlled by color-opponent mechanisms. *Vision Research, 19*, 1025–1040.

Tyndall, E. P. T. (1933). Chromaticity sensibility to wavelength difference as a function of purity. *Journal of the Optical Society of America, 23*, 15.

Werner & Wooten (1979). Opponent chromatic mechanisms: Relation to photopigments and hue naming. *Journal of the Optical Society of America, 69*, 422–434.

Williams, D. R., MacLeod, D. I. A. & Hayhoe, M. M. (1981). Punctate sensitivity of the blue-sensitive mechanism. *Vision Research, 21*, 1357–1375.

Wright, W. D. (1935). Intensity discrimination and its relation to the adaptation of the eye. *Journal of Physiology, London, 83*, 466–477.

Zaidi, Q. (1992). Parallel and serial connections between human color mechanisms. In Brannan, J. (Ed.), *Applications of parallel processing in vision* (pp. 227–259). Amsterdam: Elsevier.

*Acknowledgements*—This work was partially supported by the National Eye Institute through grants EY07556 to Q. Zaidi and EY02115 to D. Hood. Portions of this work were presented at ARVO 1988 and 1989.